August 2019

Reduced GABAergic Signaling at the Axon Initial Segment Decreases Vigilance State Transitioning

Austin John Boren

REDUCED $GABA_{ERGIC}$ SIGNALING AT THE AXON INITIAL SEGMENT DECREASES VIGILANCE STATE TRANSITIONING

By

Austin John Boren

Bachelors of Arts – Psychology
University of Nevada, Las Vegas
2016

A thesis submitted in partial fulfillment
of the requirements for the

Master of Arts - Psychology

Department of Psychology
College of Liberal Arts
The Graduate College

University of Nevada, Las Vegas
August 2019

UNLV | GRADUATE COLLEGE

Thesis Approval

The Graduate College
The University of Nevada, Las Vegas

May 10, 2019

This thesis prepared by

Austin John Boren

entitled

Reduced GABAergic Signaling at the Axon Initial Segment Decreases Vigilance State Transitioning

is approved in partial fulfillment of the requirements for the degree of

Master of Arts - Psychology
Department of Psychology

Rochelle Hines, Ph.D.
Examination Committee Chair

Kathryn Hausbeck Korgan, Ph.D.
Graduate College Dean

Dustin Hines, Ph.D.
Examination Committee Member

James Hyman, Ph.D.
Examination Committee Member

Gary Kleiger, Ph.D.
Graduate College Faculty Representative

ABSTRACT

Reduced GABAergic signaling at the axon initial segment decreases vigilance state transitioning

by

Austin John Boren

Dr. Rochelle Hines, Examination Committee Chair
Assistant Professor of Psychology
University of Nevada, Las Vegas

Sleep is a highly regulated homeostatic process that is disrupted in an estimated 50-70 million Americans. Regulation of sleep depends upon coordinated signaling of multiple neurotransmitter systems. In particular, inhibitory gamma-aminobutyric acid (GABA) signaling is required to suppress wake-active brain regions in order to initiate and maintain sleep states. GABA type A receptors ($GABA_AR$s) are ionotropic receptors with subunit compositions uniquely enriched on subcellular domains of target cells. α2 subunit-containing $GABA_AR$s are the primary target of GABA released onto the axon initial segment (AIS), a site critical for phasing the oscillatory activity of cortical cells. α2-containing $GABA_AR$s have previously been implicated in the initiation and maintenance of sleep. To determine the contribution of GABAergic singling at the AIS to regulation of sleep, we used behavioral and electroencephalographic measures to assess sleep in a mouse featuring a loss of inhibitory synapses onto the AIS (*Gabra2*-1). Reduced GABAergic input to the AIS results in a persistent increase in the delta frequency range in *Gabra2*-1 mice, suggesting an alteration in sleep regulation. Analysis of long term recordings demonstrate that *Gabra2*-1 homozygous mice spend less time asleep during

subjective night, and also have reduced vigilance state transitions. *Gabra2*-1 homozygous mice show a loss of free running rhythm when housed in constant darkness, and fail to homeostatically respond to 24 hours of sleep deprivation. These studies demonstrate a role for α2 containing $GABA_AR$s in sleep initiation, transitions, and the response to sleep challenges, providing critical information for the refinement of sleep therapies.

TABLE OF CONTENTS

ABSTRACT..... iii

LIST OF FIGURES..... vi

CHAPTER 1 INTRODUCTION 1

CHAPTER 2 REVIEW OF RELATED LITERATURE..... 6
Inhibition, γ-aminobutyric acid and γ-aminobutyric acid receptors..... 6
The axon initial segment..... 8
GABAergic contribution to sleep, circadian, and ultradian rhythms 11

CHAPTER 3 MATERIALS AND METHODS..... 15
Subjects..... 15
Genetic strategy..... 15
Western Blotting..... 15
Immunohistochemistry..... 16
Electroencephalographic surgery and data collection..... 16
Vigilance state scoring..... 17
24 hour baseline electroencephalographic assessment..... 17
Behavioral measures..... 18
Statistical analyses..... 19

CHAPTER 4 EXPERIMENTAL HYPOTHESES..... 20

CHAPTER 5 RESULTS..... 21
Reduced α2 signaling at the axon initial segment increases baseline electroencephalographic power across a 24 Hour period..... 21
Electroencephalographic alterations in Gaba2-1 homozygous mice are vigilance state specific..... 24
*Gabra*2-1 mice spend more time awake during the subjective night..... 26
*Gabra*2-1 have deficits in vigilance state transitions restricted to subjective night... 29
*Gabra*2-1 mice cannot maintain free running circadian rhythmicity and have attenuated response to sleep deprivation..... 31

CHAPTER 6 DISCUSSION AND FUTURE DIRECTIONS..... 34

CHAPTER 7 SUPPLEMTARY INFORMATION..... 39

BIBLIOGRAPHY..... 43

CURRICULUM VITAE..... 49

LIST OF FIGURES

Figure 1 Generation and characterization of the *Gabra2*-1 mutant mouse model basic phenotype……..……....22
Figure 2 Increased power in *Gabra2*-1 homozygous mice is persistent across a 24 hour period……..…23
Figure 3 *Gabra2*-1 homozygous mice have increased electroencephalographic power in the state of wake and non-rapid-eye-movement sleep restricted to specific frequency ranges……25
Figure 4 *Gabra2*-1 homozygous spend more time awake during subjective night…..27
Figure 5 *Gabra2*-1 homozygous have increased vigilance state duration and decreased transitions restricted to subjective night……..…30
Figure 6 *Gabra2*-1 homozygous mice have altered behavioral response to sleep challenges……..…33

Supplementary Figures

SI Figure 1 Generation and genotyping *Gabra2*-1 mice……...39
SI Figure 2 Hourly assessment of absolute delta power for a 24 hour period……...39
SI Figure 3 24 hour cFFT normalized to delta, theta, and gamma ……...40
SI Figure 4 Figure 4. Assessment of percent time spend in state of non-rapid-eye-movement sleep……41
SI Figure 5 Assessment of total transitions across a 24 hour period……41

Supplementary Table

SI Table 1 Results for two visual tests from modified SHIRPA screening protocols…42

CHAPTER 1

INTRODUCTION

The central nervous system (CNS) oscillates at multiple timescales allowing for temporal patterning of complex behavior. The cyclic patterning of sleep is considered to be a master oscillatory pattern as it regulates many homeostatic functions[1]. Disruptions to its progression results in primary sleep disorders impacting 50-70 million Americans while sleep disturbances are a common symptom of CNS disorders[2,3]. Homeostatic regulation of sleep depends on the establishment and maintenance of oscillatory patterns occurring on relatively long time scales, including the circadian rhythm. In humans, the circadian rhythm is an oscillation taking about 24 hours that determines the timing of sleep [4]. Misalignment of the circadian rhythm to the natural light/dark cycle results in circadian rhythm disorders[5]. While the circadian rhythm regulates the timing of the sleep/wake cycle, a shorter 90-mintue oscillation, the basic rest activity cycle (BRAC)[6], further regulates the time in which we are sleeping, delimiting the known sleep stages. Determined by the predominate electroencephalographic (EEG) signal present, sleep is divided into non-rapid-eye-movement (NR) and rapid-eye-movement sleep (R). NR sleep, consuming about 75% of our sleeping hours, is dominated by the presence of slow wave activity in the delta frequency range (0.5-4.0 Hz) representing large, highly synchronized networks of neurons [7]. In contrast R, taking up about 25% of our sleeping hours, is dominated by a high delta/theta ratio along with the presence of gamma (30-100Hz) which is associated with network activity, allowing for dreams [8]. The establishment and maintenance of oscillatory patterns essential to sleep regulation depends on GABAergic signaling inhibiting wake-promoting regions[9] at appropriate

times. There are several lines of evidence suggesting a pivotal role for GABAergic signaling in sleep onset and maintenance with the first coming from the discovery of sleep inducing drugs. Many sleep drugs were discovered without knowing their functional properties, yet later it came to light that the majority of them acted by increasing the affinity of gamma-aminobutyric-acid (GABA) to GABA receptors[10]. Further, when specific GABA receptor subtypes are render insensitive by point mutation, these compounds they lose their sedative qualities[11,12]. Lastly, it is found that increased GABAergic signaling in distinct brain regions either promotes or reduces sleep[10,13]. Taken together, these studies suggest a central role for GABA and GABA receptors in sleep and sleep regulation.

A large body of work has since demonstrated that GABAergic neurotransmission is diverse in terms of cellular origin, postsynaptic subcellular target, and molecular composition, giving rise to diverse functional implications[14–16]. One key role of GABAergic singling is the patterning of excitatory output into oscillatory states, that support specific behavioral states, including active and relaxed waking, as well as stages of sleep[17,18]. The potential to control oscillatory activity is particularly true of GABAergic contacts on the soma and axon initial segment (AIS) that exert powerful control over pyramidal cell activity by virtue of proximity to the site of action potential generation[19].

The primary target of synaptically released GABA is the ionotropic GABA type A receptor ($GABA_ARs$)[20]. Each $GABA_AR$ contains a combination of five out of 19 possible subunits: α(1-6), β(1-3), γ(1-3), δ, ε, θ, π, and ρ(1-3), resulting in 26 known human isoforms[14]. The majority of functional $GABA_ARs$ expressed in the brain are composed of

two α, two β, and one γ subunit[21]. Although subunit composition is relatively uniform amongst $GABA_AR$s, the specific subunit composition plays a significant role in determining function. α subunits are thought to be important determinants of localization and consequent function, with α1-3 subunits being enriched in receptors clustered at specific postsynaptic targets, and α4-6 enriched in extra synaptic receptors[21]. $GABA_AR$s containing the α1 subunit are found to be enriched at axo-somatic synapses postsynaptic to parvalbumin positive basket cells [22] while α2/3 containing $GABA_AR$s are enriched postsynaptic to cholecystokinin-expressing positive basket cells[15,23]. α2 containing $GABA_AR$s are also notably enriched along the AIS, postsynaptic to parvalbumin positive chandelier cells[24–26], a site thought to play a pivotal role in shaping excitatory output[27].

The advent and subsequent study of subunit selective sleep compounds suggests $GABA_AR$s containing the α2 subunit may be central to sleep regulation. Classic sleep agents such as diazepam are non-selective as they act on all benzodiazepine sensitive $GABA_AR$s including receptors containing the α1, α2, α3, or α5 subunit[28]. Interestingly, the α1/α2 selective compound zolpidem (Ambien) action alone is sufficient for inducing certain aspects of sleep. Specifically, zolpidem decreases sleep latency and increases sleep time[29,30]. In addition, selective application of zolpidem in the tuberomammillary nucleus is sufficient for the effects of zolpidem on sleep latency, and zolpidem application in the frontal cortex can reduce sleep latency in a top down fashion[30]. Further, expression of the $GABA_AR$ containing the α2 subunit has been documented in hypothalamic and pontine regions[31], including on histaminergic neurons

of the tuberomammillary nucleus[32,33] yet its precise role in sleep regulation is yet to be demonstrated.

Previous work has identified a 13 amino acid sequence within the large intracellular loop of the $GABA_AR$ α2 subunit that is essential for trafficking to the AIS[34]. Our recent study showed that the α1/3 and α2 loops have complementary interaction strengths with gephyrin and collybistin, with the α2 loop and collybistin SH3 domain having a unique high affinity interaction[35]. Based on the indication of the α2 loop in collybistin interaction and AIS localization, we generated and characterized a novel strain, *Gabra2*-1, that expresses a 13 amino acid substitution from the α1 subunit into the α2 subunit large intracellular loop(Figure 1 A)[35]. Total expression of α2 was increased in the cortex of *Gabra2*-1 mice, but collybistin was dramatically reduced (Figure 1 B). Assessment of inhibitory synapses targeting the axon initial segment revealed a loss of α2 enrichment and VGAT positive contacts (Figure 1C)[35].

In the present study we use *Gabra2*-1 mice as a tool to probe the functional impact of AIS GABAergic signaling in oscillatory activity and behavioral output, focusing on sleep architecture, homeostasis, and the response to sleep challenges. We demonstrate that reduced α2 signaling at the AIS in *Gabra2*-1 homozygous mice results in a striking increase in baseline EEG power that is maintained across the 24 hour period. Spectral analysis demonstrates that the increase in EEG power is restricted to the delta frequency ranges during the vigilance state of NREM sleep. Interestingly, this manifests as a reduction in time spent asleep during subjective night. Further, *Gabra2*-1 homozygous mice also show reduced transitions into and out of specific stages of sleep. *Gabra2*-1 homozygous mice also have altered responses to sleep challenges,

including an inability to maintain free running circadian rhythmicity in the absence of light as a zeitgeber, and a blunted homeostatic response to sleep deprivation.

CHAPTER 2

REVIEW OF RELATED LITRATURE

Inhibition, γ-aminobutyric acid and γ-aminobutyric acid receptors

First localized at nerve terminals in the 1970's using radioactive labelling and complementary electron microscope autoradiography techniques, GABA was recognized as the primary inhibitory neurotransmitter of the CNS[36]. This neurotransmitter is produced by two enzymatic reactions, GAD65 and GAD67 acting on glutamate[37]. The resulting GABA neurotransmitter is loaded into synaptic vesicles by vesicular neurotransmitter transporter (VGAT) and is then ready to be released into the synaptic cleft by presynaptic Ca^{2+} signaling.

Once GABA is released into the synaptic cleft it can act upon ionotropic as well as metabotropic GABA receptors. Discovered by professor Norman Bowery in 1981[38], metabotropic G-protein-coupled γ-aminobutyric acid, B-type ($GABA_B$) receptors, found both pre- and post-synaptically, are responsible for the tonic inhibitory action of GABA. $GABA_B$ receptors take relatively more time than other GABA receptors to act due to the time it takes for G-protein-coupled receptors to activate the necessary components of the pathway and effect downstream inhibition. When GABA binds to $GABA_B$ in presynaptic receptors it inhibits presynaptic Ca^{2+} channels effectively reducing neurotransmitter release while activation of postsynaptic $GABA_B$ receptors acts on several inward rectifying K^+ channels hyperpolarizing neurons and shunting excitatory input[39,40]. Although mutations to $GABA_B$ receptors are implicated in disease states, it is the phasic form of inhibition and its associated receptor type that is implicated in sleep disorders.

$GABA_AR$s are the primary source of phasic inhibition in the adult CNS. $GABA_AR$s have active binding sites for psychoactive drugs including benzodiazepines, barbiturates, steroids, anesthetics, and anticonvulsants[41]. $GABA_AR$s are heteropentameric ligand gated ion channels allowing Cl^- to pass through the central canal when activated. Each $GABA_AR$ is constructed from a combination of five subunits including α(1-6), β(1-3), γ(1-3), δ, ε, θ, π, and ρ(1-3)[42] with 26 human isoforms being identified thus far[42].

Signaling properties, localization, and expression of $GABA_AR$s is determined by subunit composition. When considered globally, $GABA_AR$s containing α1, β2, and γ2 subunits are the most highly expressed across all brain regions[42]. Regionally, receptors containing α1, β1, β2, and β3 subunits are homogenously expressed while receptors containing α2, α3, α4, α5, α6, γ1 and δ subunits are found to be heterogeneously expressed, primarily in the forebrain areas[41]. Allowing for precise spatial and temporal modulation of excitatory signaling, $GABA_AR$s are also differentially expressed at subcellular locations postsynaptic to specific interneurons synapsing on dendrites, axons, and the cell body[15]. Receptors containing the α1 subunit are found at most GABAergic synapses with the highest concentration at inhibitory synapses on dendrites and soma postsynaptic to parvalbumin positive basket cells[25]. Receptors containing the α2 subunit, more limited in their expression, are found to be enriched postsynaptic to chandelier cells synapsing at the AIS[43]. Analysis of subunit concentration at the synaptic level has shown that $GABA_AR$s found at extra-synaptic sites generally contain α4 or α6 subunits while receptors found at synaptic sites generally contain α1, α2, or α3[44,45]. Given the highly specialized nature of $GABA_AR$s distribution, altered inhibitory

localization and expression is thought to underlie diseases of neuronal dysregulation, highlighting the importance of discovering the signaling molecules and proteins involved in their trafficking and expression[46].

Several receptor-associated, adhesion, and scaffolding proteins are suspected to interact with $GABA_ARs$ subtypes in unique ways allowing for differential expression and localization. Although the full signaling pathway for trafficking of all $GABA_ARs$ subtypes has yet to be discovered, a few key proteins have been identified as central to this process. Gephyrin, a scaffolding protein necessary for the clustering of several receptor types including glycine receptors is found to be highly co-localized with $GABA_ARs$[47,48]. The Moss lab has demonstrated binding motifs on $GABA_ARs$ containing α1, α2, and α3 subunits for gephyrin necessary for appropriate receptor clustering[49–51]. Recent work from the Moss lab demonstrates the necessity of another scaffolding protein, collybistin, in the trafficking and clustering of $GABA_ARs$ containing the α2 subunit onto the AIS[35]. In the present study we aim to determine the contribution of $GABA_ARs$ containing the α2 subunit at the AIS to the phenomena of sleep, as this synaptic sight, discussed in the next section, is thought to be central to network functioning.

The axon initial segment

Excitatory principal neurons are the fundamental cells of neuronal communication in the CNS. These specialized cells have an atypical structure, one of asymmetry, endowing them with specialized communication properties. First proposed by Santiago Ramon y Cajal, along with the neuron doctrine, the law of dynamic polarization states that information flows along the principal neuron in only one

direction, driven by cellular polarization[52,53]. Under this paradigm, the neuron can be seen as a simple input-output device. The dendrites act as an input device, sensing a signal in the form of a chemical messenger from up-stream neurons. This signal is then transduced to the cell body. If polarity is sufficiently shifted, an action potential (AP) is fired, the signal is then transduced along the axon where the terminal buttons act as an output device. This stroke of insight by Cajal inspired generations of biologist to study and define the cellular structures, receptors, and chemical messengers underlying this fundamental principal of neuronal communication.

In landmark experiments conducted by Hodgkins and Huxley on the signaling properties of the giant squid axon, they described the principal electrical component of neuronal communication, namely the AP[54]. The 'decision point' determining if an AP is fired occurs in a specialized subcellular compartment found just distal of the axon hillock and ending at the first section of myelination, the AIS[43]. Similar to the nodes of Ranvier, the AIS is studded with ion channels allowing for rapid depolarization and repolarization. Three forms of Na^+ channels are highly enriched on the AIS including $Na_v1.1$[55], $Na_v1.2$[56], and $Na_v1.6$[57] allowing for rapid depolarization and AP initiation. K^+ channels including $K_v1.1$ and 1.2 are enriched at the AIS for rapid repolarization[58].

Modulation of AP's occurs via GABAergic interneurons synapsing at the AIS. Specifically, the chandelier cell with its striking morphology of highly branched axonal arbors are found to synapse exclusively at the AIS[59,60]. These specialized interneurons are thought to contribute to the generation of neuronal networks as their highly branched arbors reach out and synapse with hundreds of principal cells[61] at the AIS allowing them to effectively modulate the timing of AP's across neuronal networks[62]. Of

interest to the current study, chandelier cells, or axo-axonic cells, are found to have a high postsynaptic density of $GABA_A$Rs containing the α2 subunit suggesting this $GABA_A$ receptor subtype may be central to network functioning[62].

Given the significant role the AIS, axo-axonic cells, and $GABA_A$Rs containing the α2 subunit play in network functioning, disruptions to these processes are thought to underlie common disorders of the CNS. It has been demonstrated that axo-axonic synapses are reduced at the epileptic foci[63] and are thought to underlie continued dysregulated excitation in epilepsies. Further, altered axo-axonic innervation and α2 distribution are thought to disrupt the excitatory to inhibitory 'balance'[64] and contribute to schizophrenia and neurodevelopmental disorders including autism spectrum[65,66]. The full contribution of altered AIS morphology, axo-axonic cell synapsis, and distribution of $GABA_A$Rs containing the α2 subunit to these common disorders is still an open scientific question.

Very little is known about the contribution of the AIS and axo-axonic cells to the processes of sleep. Sleep is dependent and defined by specific oscillatory activity discussed in the next section. Given the role axo-axonic cells play in patterning pyramidal output into oscillatory activity, it is likely their signaling properties contribute to various oscillations of sleep. In a study conducted by Massi et. al., in 2012 they suggest axo-axonic cells and basket cells may contribute to NREM and REM sleep oscillations, including spindle and gamma oscillations[67]. It is part of the aim of this study to determine the impact of a loss of $GABA_A$Rs containing the α2 subunit at the AIS to sleep and its natural oscillatory progression.

GABAergic contribution to sleep, circadian, and ultradian rhythms

The circadian rhythm is an oscillation taking about 24 hours in humans that entrains the biological system to the environment allowing for timely behavioral output. In an elegant paper published by Aschoff in 1965, he observed circadian rhythmicity in humans under deprived conditions to understand the role of environmental input, or zeitgebers, on its cyclic duration or τ. He placed participants (including himself) in an environment lacking all zeitgebers and found that the τ of a free-running circadian rhythm in humans is an average of 25.9 hours[68]. Further, he described the impact of desynchronization, the mismatch between sleep and circadian rhythmicity, and its impact on psychological well-being. Subjects reported more positively on days in which these processes were aligned. A landmark paper published in 1982 by Borbely A.A. further refined our understating of the circadian rhythm and how it interacts with sleep. In this paper titled the '*Two process-model of sleep regulation'* it is proposed that the sleep/wake cycle (Process S) and the circadian pacemaker (Processes C) oscillate at different timescales, yet interact to define sleep wake activity. In summary it is suggested that Processes S is driven by increased sleep pressure caused by prior wakefulness and that it is entrained to the light dark cycle by Process C[4]. This model is still used today to study how Process S and C interact. Process S is established by sleep pressure which is assessed by EEG slow wave activity (SWA). Many EEG studies have shown that SWA, the hallmark of 'restorative' sleep, is modulated by prior wakefulness[69–71] with increased prior wakefulness resulting in higher levels of SWA. These data suggest that accumulation and dissipation of sleep pressure contribute to the cyclic nature of Process S. Process C is established by a complex feedback system

taking place in the suprachiasmatic nucleus which interacts with the zeitgeber light[72] The progression of Process C is assessed by levels of melatonin and core body temperature, with high levels of melatonin and reduced core body temperature indicating a higher probability of sleep initiation[73]. Described by Nathaniel Kleitman in 1963 by studying infant feeding patterns, the sleep/wake cycle is further modulated by the basic rest activity cycle (BRAC)[74]. The BRAC is an ultradian rhythm (a cycle less than a day and greater than an hour) that determines our activity level while awake and drives the progression of sleep stages while asleep[6]. That is the progression from non-rapid-eye-movement (NREM) to rapid-eye-movement sleep (REM), occurring 6-9 times a night. The interaction of these exogenously and endogenously generated cycles allow for appropriate behaviors responses at appropriate times.

Driven by these early studies, biologists have worked to understand the regions of the brain and neuronal progenitors of sleep. Sleep is a brain-wide process with a few key areas and neuronal types contributing to its onset and maintenance. The hypothalamus houses most of the regions thought to control vigilance, projecting their signal across the cortex to promote wakefulness or being suppressed to induce sleep. Within the hypothalamus, the ventrolateral preoptic nucleus (VLPO) projects onto the tuberomammillary nucleus (TMN). The VLPO houses GABAergic neurons which increase their firing rate at sleep onset[75]. The TMN houses histaminergic neurons, which when inhibited by the VLPO no longer release histamine, a wake promoting neurotransmitter, across the cortex allowing for sleep[10]. Other areas including the pedunculopontine and laterodorsal tegmental nuclei, housing cholinergic neurons, which act via another wake promoting neurotransmitter acetylcholine, are found to be

inhibited during sleep as they have been shown to be inactive during times of NREM[76]. Other distributed regions work in concert with the VLPO to inhibit wake promoting areas allowing humans to fall asleep in mere minutes. This observation led to Saper's 'flip-flop' model of sleep onset[77]. This model suggests reciprocal inhibition from several sleep promoting areas creates an integrated network that can be turned off rapidly for quick vigilance state transitions.

Given that all of the above mentioned processes depend on GABAergic inhibition, it has long been a challenge to discover the contribution of $GABA_AR$ subtypes to sleep. Classic sleep drugs including benzodiazepines are positive allosteric modulators, increasing GABA's action on $GABA_ARs$, inducing sedation and sleep. Although the action of these classic sleep compounds indicates that GABAergic signaling is central to sleep, they do not inform us about receptor subtype contribution as they act on all benzodiazepine sensitive $GABA_AR$ including α1, α2, α3, and α5[28]. The discovery of selective sleep compounds has begun to reveal the specific contribution of $GABA_ARs$ subunits to sleep. The α1/α2 selective compound Zolpidem (Ambien) is the most prescribe sleep medication in the United States. This drug is known to decrease sleep latency and increase NREM time[78]. Clarifying the action of zolpidem, studies have shown an enrichment of $GABA_ARs$ containing the α1/α2 subunit in the TMN[79,80]. Further, an electrophysiological study from Sergeeva's lab demonstrated the necessary action of α1/α2 in the TMN for the action of benzodiazepines[81]. Given the selective action of zolpidem, evidence that $GABA_ARs$ containing the α2 subunit are enriched in the TMN, and that they contribute significantly to benzodiazepine's action in the TMN, we are currently using IHC to investigate the colocalization of α2 with histaminergic

neurons in the TMN as this may be mechanistic to sleep disturbances observed in the *Gabra*2-1 mouse model.

CHAPTER 3

MATERIALS AND METHODS

Subjects

Male mice bread at UNLV were group housed under a 12 hour light cycle (0700; lights on), constant temperature, and access to food and water *ad libitum*. All animal studies were performed under protocols approved by the Institutional Animal Care and Use Committee of University of Nevada Las Vegas.

Genetic strategy

The *Gabra2*-1 mouse was generated by substitution of amino acids 358-375 from the large intracellular loop spanning transmembrane 3 and 4 of the $GABA_ARs$ containing the α2 subunit with those of $GABA_ARs$ containing the α1 subunit using homologous recombination in ES cells (Figure 1 A). Offspring were probed for the transgene using PCR with primers spanning the intronic region containing the remaining loxP site(SI Figure 1 A). Nontransgenic litter mates were used as controls in all experiments.

Western blotting

Rapidly harvested whole brain tissue was homogenized in TEEN buffer (50mM Tris-HCL, 1mM EGTA, 150mM NaCl) with the addition of a protease inhibitor from Roche Applied Science. Resulting protein concentration was determined by BCA assay (Pierce). In preparation for blotting, samples were heated to 65°C in SDS page sample buffer with 10% ß-mercaptoethanol for 15 minutes and subject to SDS page

procedures. Resulting western blot signal were detected using ECL. Quantification of specific protein levels were determined by densitometry when normalized to actin densitometry results utilizing image J software.

Immunohistochemistry

For histology, mice were transcardially perfused with periodate lysine paraformaldehyde (PFA) fixative solution. Following PFA fixation, brains were sectioned at the thickness of 30um with a cryostat and incubated in blocking solution (2.5% Bovine Serum Albumin, 5% Normal Goat Serum, 0.1% triton-X, 0.02% sodium azide in PBS) for 45 minutes. Sections were then incubated in primary antibody diluted in modified blocking solution (2% Normal Goat Serum) overnight at 4°C. Following washing, sections were then incubated in secondary antibody diluted in modified blocking solution for 1 hour at room temperature.

Electroencephalographic surgery and data collection

Mice were implanted with chronic electroencephalographic (EEG) devices under isoflurane anesthesia. Two cortical EEG electrodes (stainless-steel screws) were placed in the frontal and parietal areas. Reference and ground electrodes are placed caudally. EMG electrodes were placed bilaterally in the dorsal nuchal musculature. All electrodes were soldered to an EEG/EMG headmount (Pinnacle Technology) which was then anchored to the EEG, reference, and ground electrodes with dental cement. The mice were sutured, given a bolus of lactated ringer solution, individually housed, and monitored for pain during recovery. 48 hours prior to data collection mice were

habituated to circular Plexiglas recording chambers (Pinnacle Technology) with a preamplifier connecting the chronic headmounts to a data acquisition device (Pinnacle Technology) via a micro-connector. During data collection, the electrical signal was acquired and stored for later offline analysis by a computer-based system using Sirena Acquisition software (Pinnacle Technology). EEG was sampled at a resolution of 250Hz and band passed at 100Hz.

Vigilance state scoring

Ongoing vigilance was determined by assessment of EEG records in part by the software SleepSign for Animals (KESSEI COMTEC CO.) Each EEG record was binned in 8 second epochs and then screened using the following thresholding parameters: high EMG integral to detect wake (W), high FFT delta_power to detect non-rapid-eye movement sleep (NR), and high FFT theta_ratio to detect rapid-eye-movement sleep (REM). Resulting analysis (~90% accurate) was then confirmed by an expert in vigilance-state scoring who visualized each 8s epoch to determine the sate based on the following parameters: W was determined by high frequency and low amplitude EEG activity accompanied by high EMG activity, NR by low frequency and high amplitude EEG activity with little to no EMG activity, and REM by high frequency and low amplitude EEG activity with no EMG activity. Epochs with non-gaussian waveform were discarded as artifact. No file contained more than 1% artifact.

24 hour baseline electroencephalographic assessment

EEG recordings were made after habituation in chambers as described above. Spectrograms were generated from text files using a custom script for MATLAB. To plot relative power in frequency ranges from 0-30Hz, variance was reduced amongst surgical implants by normalization to the average from 0-100Hz within animal for a given analysis period (24 hours, ZT 12-0, and ZT 12-24). To plot vigilance state dependent relative power, data was normalized within animal to the average power from 0-100Hz of the vigilance state being assessed (W, NR, or R). Amount of time spent in each vigilance state is expressed as a percent of the total analysis time (24 hours, ZT 12-0, and ZT 12-24). A bout is defined as contiguous epochs scored as the same vigilance state while a transition is defined by a switch amongst ongoing vigilance state.

Behavioral measures

For activity analysis, diurnally entrained mice were individually housed in metabolic activity chambers allowing for measurement of activity by beam break. Activity was measured for a total of 28 days. For the first 14 days mice where kept under diurnal conditions. On day 15 through day 28 mice were housed under constant darkness conditions to measure free running circadian rhythmicity. Visual placement tasks were created using the modified SHIRPA protocol. For sleep deprivation (SD) measures, mice underwent EEG/EMG surgery and were allowed to recover as described above. Prior to experimental recordings animals were habituated to recording chambers for 48 hours (days 1 & 2) as described above. Baseline recordings began at zeitgeber time (ZT) 0 (0700/light onset) on the third day and ended at ZT 0 on the fourth day. Beginning at ZT 0 on the fourth day animals underwent SD for 24 hours using the

gentile handling method. As previously described[71] gentile handling protocols were initiated when animals began to display a sleeping posture (no movement and lowered head). Gentile handling procedures induced sleep disruption by introduction of novel objects, tapping on the cage, or gentile touch with an inflated surgical glove. These procedures were used to reduce stress caused by directly touching the animals. The recovery period began with cessation of SD procedures at ZT 0 on the fifth day. Recovery recordings were made for a total of 24 hours (day 5) allowing for sleep *ad libitum.* A simplified timeline is provided below. Data was scored for vigilance states as described above.

Days 1 & 2	Day 3	Day 4	Day 5
Recording chamber habituation	24 hour baseline	24 hour sleep deprivation	24 hour homeostatic sleep response

Sleep deprivation experimental timeline

Statistical analyses

Statistical analyses were performed using SigmaPlot 12.5 software. Differences amongst cFFT plots, vigilance state percent time analysis, and transition assessment were determined by within-subject repeated measure two-way ANOVA. Total transitions during the ZT 0-12 and ZT 12-24 were assessed by one-way ANOVA. Significant main effects and interactions were further examined using Bonferroni t-test *post hoc* analysis. The significance threshold for all test was set at 0.05.

CHAPTER 4

EXPERIMENTAL HYPOTHESES

1. **To test the hypothesis that reduced α2 signaling at the AIS will impact baseline electroencephalographic activity.** Evidence suggests α2 signaling at the AIS is central to the patterning of excitatory pyramidal output into oscillatory states. cFFT and spectral assessment of 24 hour EEG recordings will allow for the determination of the impact of a loss of α2 at the AIS to the generation of specific oscillatory states which can be correlated to behavioral states.

2. **To test the hypothesis that reduced α2 signaling at the AIS will result in abnormal sleep architecture.** Sleep homeostasis depends on integration of neuronal networks across CNS regions. Given the localization of α2 at the AIS allowing for modulation of AP initiation, we suspect a reduction in expression will disrupt homeostatic progression of sleep. Sleep scoring of 24 hour EEG recordings will allow for the analysis of sleep architecture across the circadian cycle.

3. **To test the hypothesis that reduced α2 signaling at the AIS will alter homeostatic response to sleep challenges.** Finally, if α2 contributes to the homeostatic regulation of sleep as suspected, we expect to find an altered homeostatic response to sleep challenges. Light and sleep deprivation will allow us to test this at the level of the circadian rhythm and homeostatic regulation of sleep pressure.

CHAPTER 5

RESULTS

Reduced α2 signaling at the axon initial segment increases baseline electroencephalographic power across a 24 Hour period

Previous analysis of EEG recordings made in adult *Gabra2*-1 homozygous mice revealed an increase of power in the delta frequency range (0.5-4Hz) over the course of a short recording period[35]. Given this, our first goal was to elucidate if the observed increase of delta power in *Gabra2*-1 homozygous mice is present throughout the sleep/wake cycle. To answer this question, we examined a 24 hour period of continuous EEG recordings made from freely moving wildtype, *Gabra2*-1 heterozygous, and homozygous mice. Qualitative spectrograms representing individual 24 hour baseline EEG records (Figure 2 A-C) suggested that *Gabra2*-1 homozygous mice have increased power in low frequency ranges. To assess this quantitatively, we applied a cFFT to the EEG data allowing us to plot relative power in frequencies ranging from 0-30Hz for the entire 24 hour recording period (Figure 2 D). While the *Gabra2*-1 heterozygous mice had significantly increased power when compared to wildtype controls in a very limited set of frequencies (genotype x time interaction P = <0.01; Bonferroni post hoc $p \leq 0.05$ from 3.4-3.9Hz), the homozygous mice displayed significantly increased power in a broader range of frequencies from 0.48-6.3Hz (genotype x time interaction <0.01; Bonferroni post hoc $p \leq 0.05$ from 3.4-3.9Hz), covering all of the delta frequency band and low end theta. Low frequency oscillations are associated with sleep[4,82], so next we examined if the increased delta power in *Gabra2*-1 homozygous mice follows circadian patterning with respect to

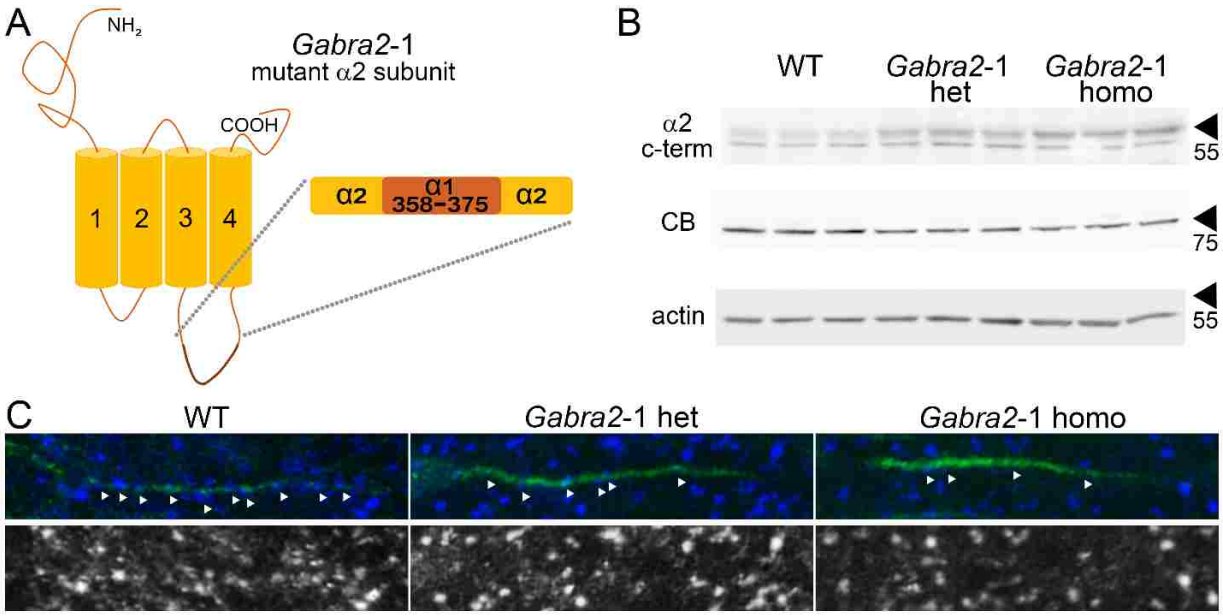

Figure 1. Generation and characterization of the *Gabra2*-1 mutant mouse model basic phenotype.

A. Cartoon depicting the large intercellular loop spanning transmembranes 3 and 4 of GABA type A receptor in which amino acid residues 358-375 of the α2 loop are replaced with the corresponding sequence from the α1 loop reducing collybistins affinity for the mutant receptor. B. Cortical extracts from wildtype, *Gabra2*-1 heterozygous, and homozygous mice were subjected to western blotting with antibodies raised against α2 c-terminus, collybisitin (CB), and internal control actin. C. Adult wildtype, *Gabra2*-1 heterozygous, and homozygous mice frontal cortex sections subjected to immunohistochemistry with antibodies raised against neurofascin to visualized the axon initial segment and VGAT to visualize inhibitory presynaptic markers (top overlay; bottom VGAT only)

photoentrainment. To answer this question, we next plotted cFFT's of the 24 hour EEG recordings parsed with respect to the circadian time periods (Figure 2 E & F). The EEG recordings were made from mice entrained to a 12 hour light cycle (0700/lights on), and as such, subjective night (lights on) is defined as zeitgeber time (ZT) 0-12 and subjective day (1900/lights off) as ZT12-24. This analysis revealed the *Gabra2*-1 homozygous mice had increased power in low end frequencies over the wildtype controls irrespective of the circadian time period (for hourly assessment of absolute

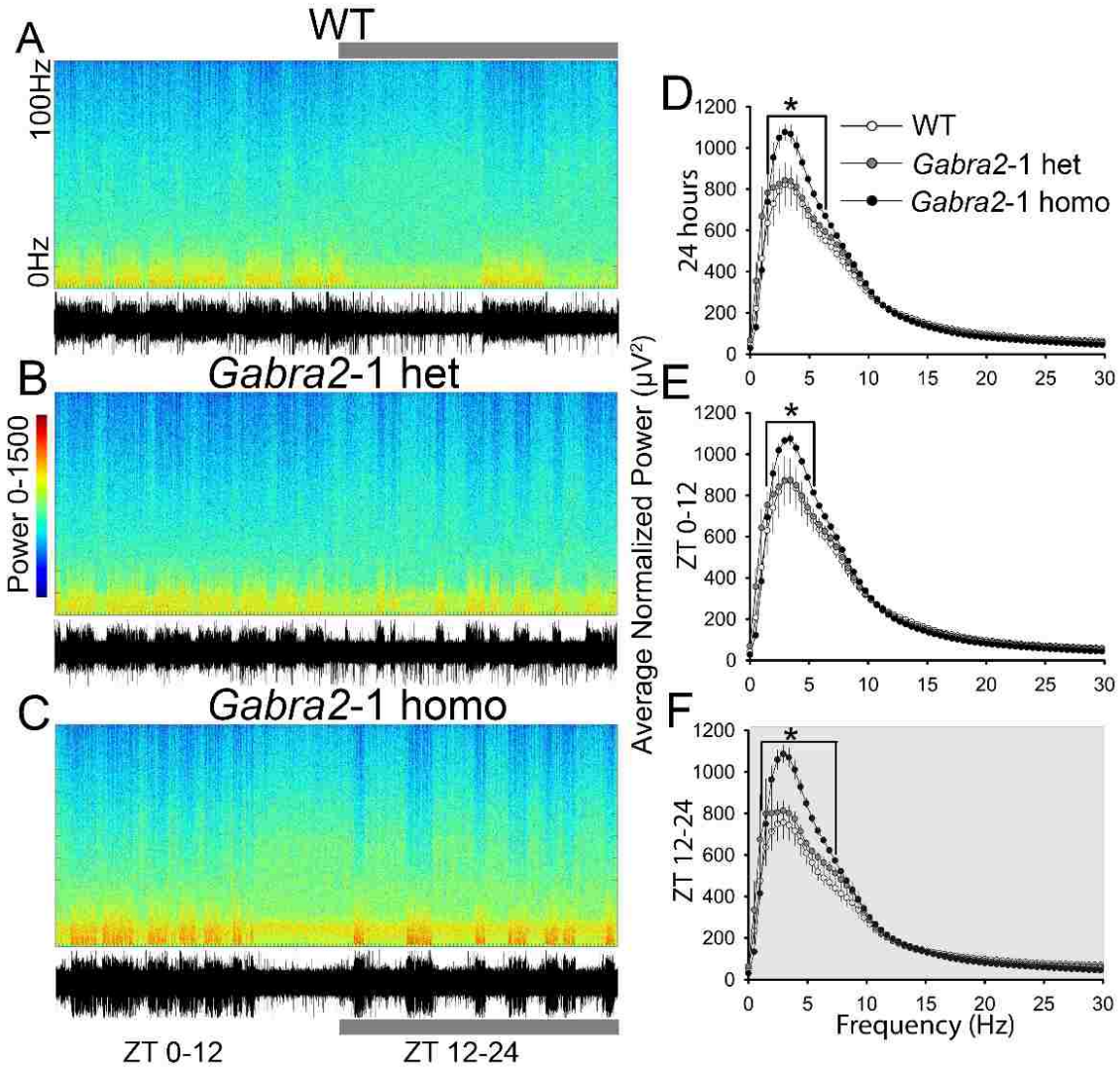

Figure 2. Increased power in *Gabra2*-1 homozygous mice is persistent across a 24 hour period.

A-C. Representative spectrograms (top) and raw traces (bottom) of 24 hour electroencephalographic (EEG) recordings made in freely moving wildtype (A), heterozygous (B), and homozygous (C) *Gabra2*-1 mice. Zeitgeber time (ZT) 0-12 is the light period (0700-1900) while ZT 12-24 is the dark period (1900-0700) indicated by the grey bar. D. A cumulative fast Fourier transformation (cFFT) applied to 24 hours EEG data shows increased power in *Gabra2*-1 homozygous (LS mean 287.789 ± 7.838) over wildtype (LS mean 258.869 ± 7.838) in low frequencies (LS mean het – 271.731 ± 7.011; genotype x frequency interaction <0.001). E & F. cFFTs of 24 hour EEG recordings parsed into ZT 0-12 (E; LS means; WT – 245.618 ± 7.604; het – 264.703 ± 6.801; homo – 288.289 ± 7.604; genotype x frequency interaction <0.001) and ZT 12-24 (D; LS Means; WT – 269.787 ± 7.901; het – 278.293 ± 7.067; homo – 289.630 ± 7.901; genotype x frequency interaction p = <0.001) suggests increased power in *Gabra2*-1 homozygous mice is maintained across subjective day and night. n = 4 to 5 per genotype, values listed are mean ± standard error, p values from repeated measures ANOVA, post hoc Bonferroni; * = ⩽0.05, ** = ⩽0.005, *** = <0.001.

delta power see SI Figure 2). These observations demonstrate that *Gabra2*-1 homozygous mice have persistently increased delta power across the 24 hour period. Collectively, these initial analyses suggested *Gabra2*-1 heterozygous mice have similar power to wildtype controls while homozygous mice have a persistent increase in delta that is not impacted by salient circadian cues.

Electroencephalographic alterations in *Gabra*2-1 homozygous mice are vigilance state specific

Given that we did not observe circadian specific alterations in delta power in *Gabra2*-1 mice, we next wished to examine if these alterations were vigilance state specific as delta frequencies are a necessary component of NR sleep[83]. To explore vigilance specificity of the EEG power alterations, we next scored each 8 second epoch of EEG data as corresponding to a state of wake (W), non-rapid-eye-movement sleep (NR), or rapid-eye-movement sleep (R) determined by the characteristics and relationship amongst the EEG/EMG signal for the given epoch (Materials & Methods). Qualitative visualization of raw traces of each vigilance state type (Figure 3 A) suggested *Gabra2*-1 animals may have altered spectral characteristics in each of these states. To test this observation, we plotted cFFT's of the EEG data from 0-30Hz with respect to vigilance state (Figure 3 B-D). Strikingly the homozygous mice displayed increased power in limited yet distinct frequency ranges for each vigilance type. To determine the specific frequency ranges impacted, we next parsed the data into relative frequency bands and plotted with respect to the vigilance state (Figure 3 E-G).

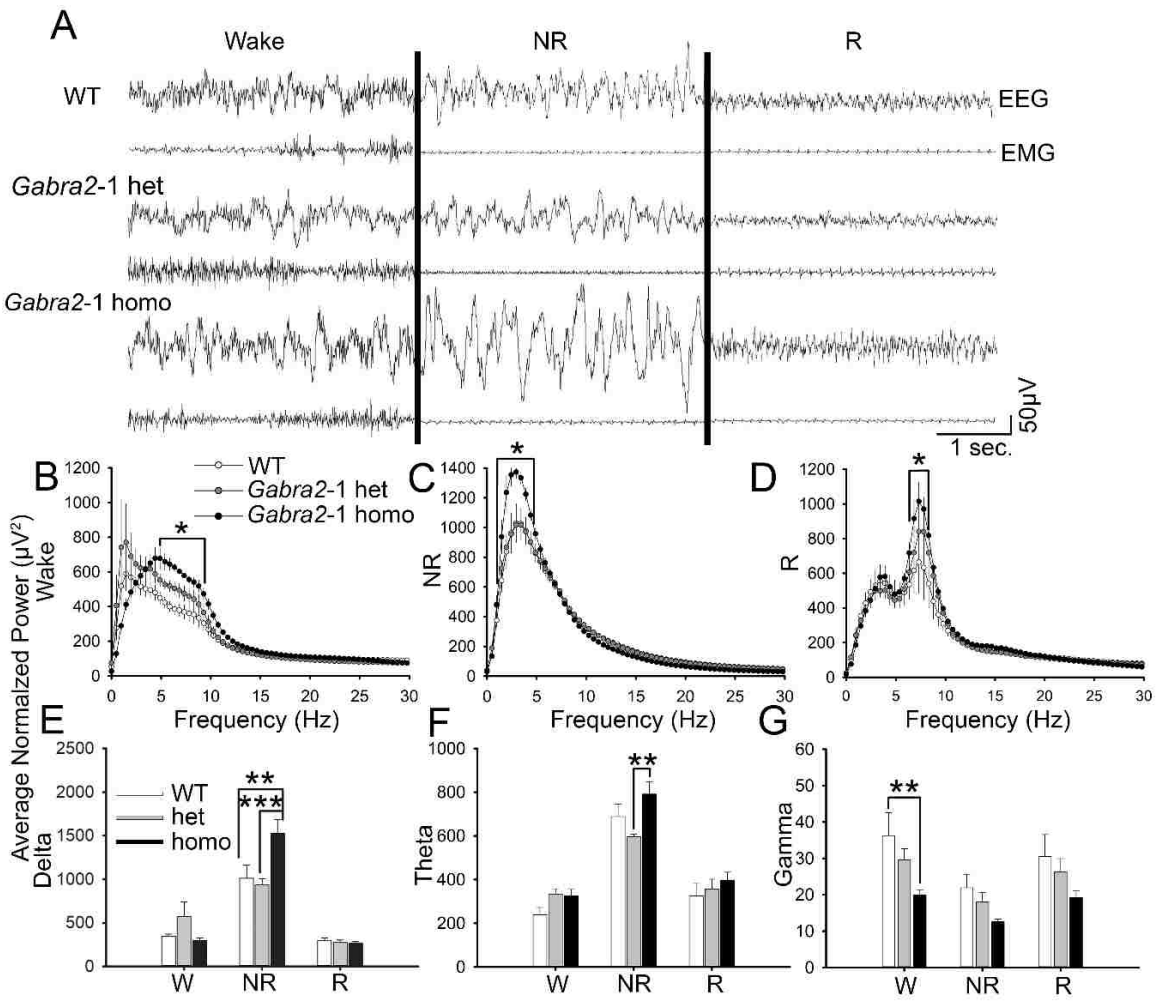

Figure 3. *Gabra2*-1 homozygous mice have increased electroencephalographic power in the state of wake and non-rapid-eye-movement sleep restricted to specific frequency ranges.

A. 4 second representative electroencephalographic (EEG) and electromyographic traces from wildtype, heterozygous, and homozygous *Gabra2*-1 mice scored as a state of wake (W), non-rapid-eye-movement sleep (NR), or rapid-eye-movement sleep (R). B-D. Cumulative fast Fourier transformation (cFFT) of 24 hours EEG data parsed with respect to vigilance state reveals the power structure of epochs scored as W (B; LS means; WT – 214.339 ± 10.684; het – 243.179 ± 9.556; homo – 254.766 ± 10.684; genotype x frequency interaction $p < 0.001$), NR (C; LS means; WT – 287.847 ± 5.098; het – 291.478 ± 4.560; homo 306.632 ± 5.098; genotype x frequency interaction $P < 0.001$), or R (D; LS means; WT – 234.160 ± 10.084; het – 242.182 ± 9.020; homo – 263.739 ± 10.084; genotype x frequency interaction $p = 0.007$). E-G. Spectral analysis of EEG data parsed with respect to vigilance state for a 24 hour period demonstrates *Gabra2*–1 homozygous mice have increased δ power (0.4-5Hz) restricted to the state of NR (E; LS means; WT – 550.896 ± 52.403; het – 592.037 ± 46.871; homo – 696.291 ± 52.403) and decreased γ power restricted to the state of W (G; WT – 29.580 ± 3.671; het – 24.656 ±3.283; homo 17.291 ± 3.671) while other relevant frequency bands including theta (F; WT – 417.148 ± 2.899; het – 428.276 ± 18.692; homo – 504.932 ±20.899) are non-significant when compared to controls (for normalization variations see supplemental figure 3). n = 4 to 5 per genotype, values listed are mean ± standard error, p values from repeated measures ANOVA, post hoc Bonferroni; * = ⩽0.05, ** = ⩽0.005, *** = <0.001.

Frequency band ranges in this study are defined as follows: delta (0.5-4 Hz), theta (4-12 Hz), alpha (12-18 Hz), beta 18-30 Hz), and gamma (30-100 Hz). This analysis allowed us to discover that the *Gabra2*-1 homozygous mice had increased power in the delta frequency ranges restricted to the state of NR (Figure 3 E) accompanied by a by a decrease in gamma power restricted to periods of W (Figure 3 G; for spectral analysis of vigilance states when normalized to all band variations see SI Figure 3). More broadly, these findings suggest that *Gabra2*-1 homozygous mice have altered EEG power during both wake and sleep, but that these alterations are restricted to specific frequencies.

Gabra2-1 mice spend more time awake during the subjective night

In light of the observation that *Gabra2*-1 homozygous mice had increased delta power restricted to the state of NR we hypothesized that they would have altered structural organization of sleep, or sleep architecture. To test this hypothesis, we individually housed diurnally entrained mice in metabolic activity chambers in which activity is chronically measured by beam break. Over the course of 14 days we observed an increase in *Gabra2*-1 homozygous activity during ZT 0-12 (Figure 4 A-B). In addition, we observed a sharp increase in activity one-hour post and prior to the day/night transition (Figure 4 C). Activity can act as a proxy for wakefulness thus these data suggests *Gabra2*-1 homozygous mice have increased time awake during ZT 0-12 (subjective night). Activity based assessment is limited by the fact that it cannot detect subtle vigilance states such as quiet wakefulness, when the mouse is awake but not moving. To mitigate this confound we next examined EEG records, the 'gold standard'

for determining ongoing vigilance[99]. Subsequent examination of data scored for vigilance (Materials & Methods) reveled the percent time animals spent in each

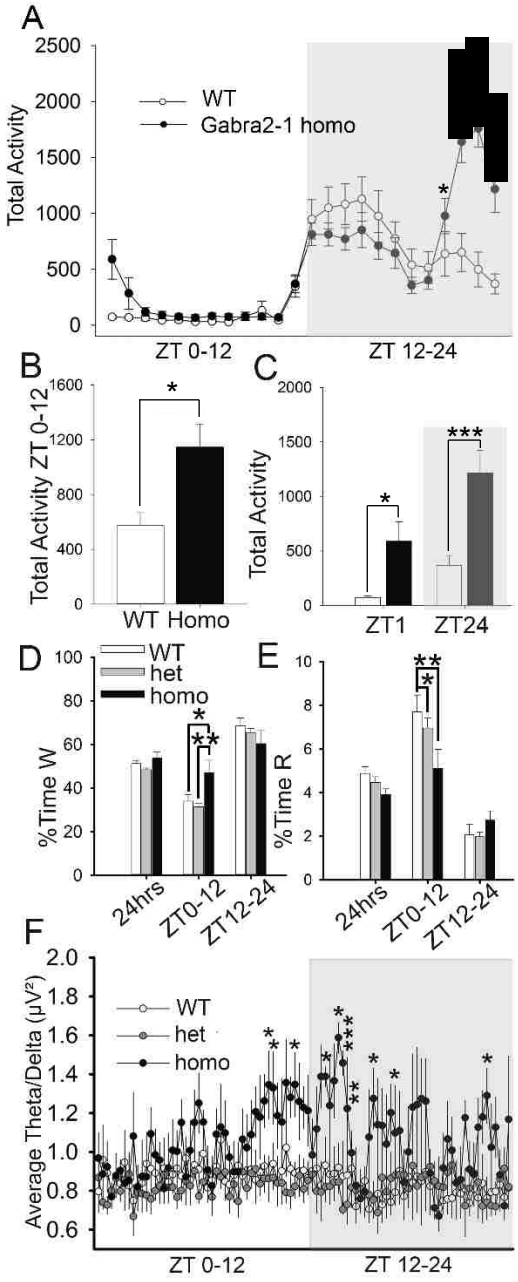

Figure 4. *Gabra2*-1 homozygous spend more time awake during subjective night.

A. 24 hour plot representing 14 days activity from diurnally entrained wildtype, and homozygous *Gabra2*-1 mice individually housed in metabolic activity chambers under diurnal conditions. B. Assessment of total activity during zeitgeber time (ZT) 0-12 (subjective night). C. Assessment of total activity during ZT 1 and ZT 24. D & E. Analysis of percent (%) time spent in a state of wake (W) (D; LS means; WT – 51.281 ± 1.760; het – 48.419 ± 1.574; homo – 53.747 ± 1.760), or rapid-eye-movement sleep (R) (E; LS means; WT – 4.886 ± 0.283; het – 4.470 ± 0.253; homo – 3.923 ± 0.283) over 24 hours, ZT 0-12, or ZT 12-24 demonstrates *Gabra2*-1 homozygous mice spend more time awake during subjective night (NR represented in supplemental figure 4). F. Ratio of theta/delta power binned every 15 minutes to examine regulation of frequency bands associated with vigilance state transitions (LS means; WT – 0.853 ± 0.0690; het – 0.824 ± 0.0617; homo – 1.061 ± 0.0691; genotype x frequency interaction p = 0.012). n = 4 to 5 per genotype, values listed are mean ± standard error, p values from one way ANOVA or repeated measures ANOVA, post hoc Bonferroni, * = ⩽0.05, ** = ⩽ 0.005, *** = <0.001.

vigilance state across ZT 0-12 and ZT 12-24 (Figure 4 D & E) is altered, again suggest disrupted sleep architecture in *Gabra2*-1 homozygous mice. Specifically, the EEG assessment revealed *Gabra2*-1 heterozygous and homozygous mice spend similar amounts of time in each vigilance state across the 24 hour period, yet the homozygous mice spend significantly more time awake during subjective night (Figure 4 D ZT 0-12) at the expense of time in R (Figure 4 E ZT 0-12). Further, this observation is restricted to subjective night as *Gabra2*-1 animals spend similar time in each vigilance state during subjective day (Figure 4 D & F; ZT 12-24; NR represented in SI figure 4).

Driven by our observations that *Gabra2*-1 homozygous mice have reduced sleep restricted to subjective night we next wished to examine biological indicators of appropriate vigilance regulation. While prominent delta power is associated with NR sleep, high theta frequencies are associated with wake and transitioning amongst these states[82,85]. To understand the ongoing relationship amongst these signals modulating vigilance and transitioning in the mice, we next plotted a ratio of theta to delta frequencies when binned every 15 minutes over a 24 hour period (Figure 4 F). This analysis suggested that *Gabra2*-1 homozygous mice do not regulate the relationship amongst these behaviorally relevant frequency ranges in the same way as the wildtype littermates, with aberration appearing around the transition from subjective day to night (Figure 4 F). To confirm these findings are not an artifact of an inability to detect photoperiods due to visual impairment, two visual placement task from the modified SHIRPA screening protocols (http://empress.har.mrc.ac.uk/browse/?sop_id = 10_002_0) were preformed (Materials & Methods) demonstrating normal vision in both heterozygous and homozygous *Gabra2*-1 mice (SI table 1). These findings suggest

Gabra2-1 homozygous mice have altered sleep architecture during subjective night that may be driven by dysregulation of global brain states.

Gabra2-1 have deficits in vigilance state transitions restricted to subjective night

Encouraged by our observations of decreased time asleep during subjective night and deficits in regulation of brain states associated with vigilance state transitioning in *Gabra2*-1 homozygous mice, we next wished to examine vigilance state duration and transitions across a 24 hour period. These measures are indicators of sleep quality as they are disrupted when the suprachiasmatic nuclei is lesioned[86] or when animals are housed under continuous bright light[87]. Qualitative examination of 24 hour actograms (Figure 5 A) suggested altered vigilance state bout duration (time between transitions) and total transitions (vigilance shift from W to NR, NR to W, NR to R, or R to NR.) To quantitatively assess this observation, we determined the mean bout duration of W, NR, and R with respect to subjective day and night (Figure 5 B & C). These data show a striking increase in mean bout duration of W in *Gabra2*-1 homozygous mice during subjective night (Figure 5 B) which is not present during subjective day (Figure 5 C). To corroborate these data we next plotted the total number of transitions occurring over 24 hours (SI Figure 4), and within ZT 0-12 and ZT 12-24 (Figure 5 D & E) as we would expect decreased transitions to accompany an increase in mean bout duration. These data show *Gabra2*-1 homozygous mice have decreased total transitions over 24 hours (SI Figure 4), yet these deficits are restricted to subjective night (Figure 5 D & E). To further clarify the microarchitecture of the observed deficits in transitioning during the light phase we next examined the number of transitions occurring during ZT 0-12 and ZT 12-24 by transition type (Figure 5 F & G). This analysis

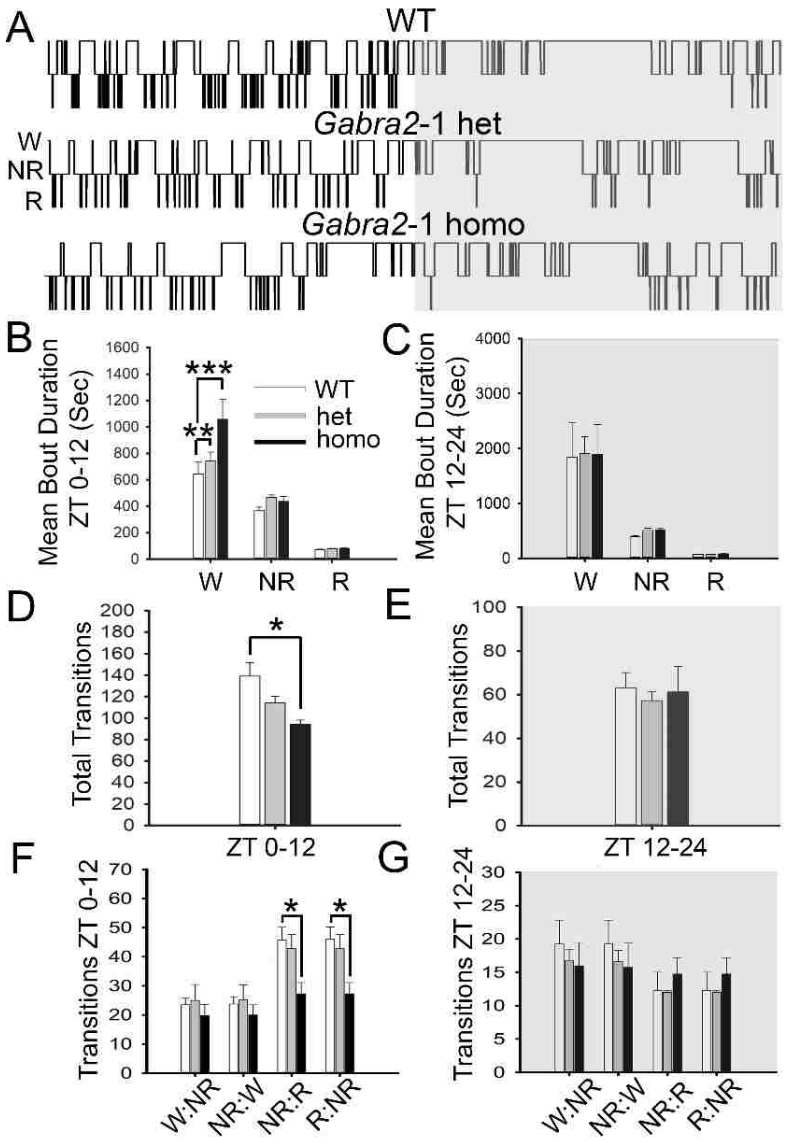

Figure 5. *Gabra2*-1 homozygous have increased vigilance state duration and decreased transitions restricted to subjective night.

A. Representative hypnograms of 24 hour electroencephalographic (EEG) recordings parsed into 8 second epochs and scored as a state of wake (W), non-rapid-eye-movement sleep (NR), or rapid-eye-movement sleep (R) from wildtype, heterozygous, and homozygous *Gabra2*-1 mice. B & C. Mean duration of vigilance state bout scored as W, NR, or R for zeitgeber time (ZT) 0-12 (B; LS means; WT – 360.333 ± 40.046; het – 429.800 ± 35.818; homo – 524.333 ±40.046) and ZT 12-24 (C; LS means WT – 769.167 ± 170.414; het 828.867 ± 152.423; homo 832.583 ± 170.414). D & E. Summation of all vigilance state transition types for ZT 0-12 (D; LS means; WT – 202.000 ± 10.840; het – 171.600 ± 4.366; homo – 155.500 ± 10.82) and ZT 12-24 (E; LS means; WT – 63.000 ± 7.141; het 57.400 ± 3.868; homo – 61.250 ± 11.643) shows an overall deficit in *Gabra2*-1 homozygous mice transitions during the light phase. F & G. Examination of transitions by type during ZT 12-0 (F; LS means; WT – 34.750 ± 3.705; het – 33.920 ± 3.314; homo 23.563 ± 3.705) and ZT 12-24 (G; LS means; WT – 15.750 ± 1.991; het – 14.350 ± 1.781; homo – 15.313 ± 1.991). n = 4 to 5 per genotype, values listed are mean ± standard error, p values from one way ANOVA or repeated measures ANOVA, post hoc Bonferroni, * = ⩽0.05, ** = ⩽0.005, *** = <0.001.

supported our findings that transitioning is reduced during subjective night and revealed that this reduction is specific to the transition into and out of R (Figure 5 F). Taken together, our findings demonstrate that the *Gabra2*-1 homozygous mice have reduced time asleep during subjective night that is manifested as a reduction in behavioral transitions during sleep, specifically when transitioning into and out of NR sleep.

*Gabra*2-1 mice cannot maintain free running circadian rhythmicity and have attenuated response to sleep deprivation.

Next, we undertook two experiments, each introducing a sleep challenge, to determine the homeostatic sleep response of *Gabra2*-1 mice. In the first experiment we individually housed diurnally entrained mice in metabolic activity chambers allowing for the chronic tracking of movement by beam break. Initially baseline activity was monitored under diurnal conditions (L/D; Figure 6 A top actograms) for 14 days followed by the introduction of constant darkness (D/D; Figure 6 A bottom actograms) for 14 days. Qualitative assessment suggests the wildtype group maintained a free running circadian rhythm for the entirety of the D/D portion of the experiment[88] while the *Gabra2*-1 homozygous mice displayed an aberrant increase in activity on the first light period in which darkness was introduced (Figure 6 A bottom right actogram). A quantitative comparison of total activity during subjective night under L/D and D/D conditions (Figure 6 B) demonstrated the loss of light, the most salient environmental zeitgeber, causes a significant increase in activity in *Gabra2*-1 homozygous mice during ZT 0-12. Encouraged by our findings that *Gabra2*-1 homozygous mice are unable to maintain a free running circadian rhythm in the absence of light, we next set out to

examine how these animals would respond to a severe sleep challenge such as total sleep deprivation (SD). To determine the homeostatic response to sleep loss, we recorded EEG while inducing SD by gentile handling methods for a total of 24 hours (Materials & Methods; timeline Figure 6 C; representative spectrograms Figure 6 D). On the day of 24 hours sleep deprivation *Gabra2*-1 mice had a similar response to the procedures as the wildtype group, maintaining a state of W for ~95% of the time (Figure 6 E), yet had a very different homeostatic response on the recovery day. Analysis of percent time pre/post sleep deprivation reveal an expected decrease in time spent awake in the wildtype group which is compensated for by an increase in time spent in the stage of NR and R (Figure F G; pre/post SD x vigilance state interaction $p = 0.002$) while both *Gabra2*-1 heterozygous and homozygous show no significant changes (Figure 6 G & H). Taken together these findings demonstrate *Gabra2*-1 homozygous mice have an inability to homeostatically respond to sleep challenges.

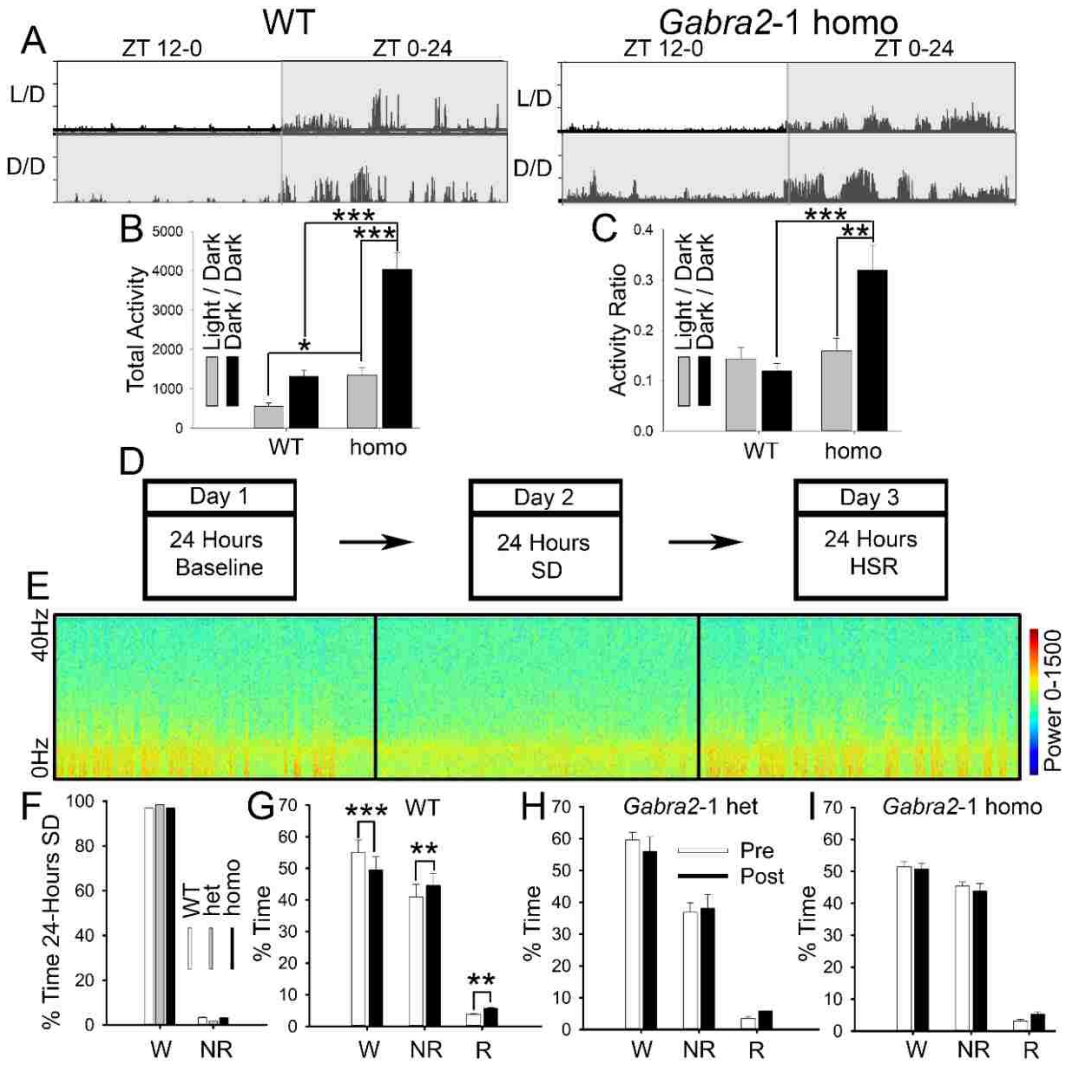

Figure 6. *Gabra2*-1 homozygous mice have altered behavioral response to sleep challenges.

A. Representative actograms of 24 hours activity under diurnal (L/D; top trace) and total darkness conditions (D/D; bottom trace) from wildtype (left) and *Gabra2*-1 homozygous (right) mice. B. Comparison of total activity under diurnal conditions (grey bars) and constant darkness. C. Comparison of activity ratio under diurnal conditions (grey bars) and constant darkness. D. Sleep deprivation (SD) timeline. E. Representative wildtype spectrograms from each day of SD experiment. F. Quantification of percent time spent in a state of wake (W) or non-rapid-eye-movement sleep (NR) representing 24 hours of SD. G-I. Quantification of percent time spend in a state of W, NR, or rapid-eye-movement sleep (R) pre and post SD for wildtype (G; LS means; W – 52.383 ± 3.893; NR – 42.800 ± 3.893; R – 4.788 ± 3.893), heterozygous (H; LS means; W 57.879 ± 3.578; NR – 37.500 ± 3.578; R – 4.621 ± 3.578), and *Gabra2*-1 homozygous mice (I; LS means; W – 51.112 ± 1.817; NR – 44.613 ± 1.817; R – 4.272 ± 1.817). SD data n = 2 per genotype; values listed are mean ± standard error; p values from repeated measures ANOVA, post hoc Bonferroni; * = ⩽0.05, ** = ⩽0.005, *** = <0.001

CHAPTER 6

DISSCUSSION AND FUTURE DIRECTIONS

Despite the significant role of $GABA_ARs$ containing the α2 subunit found at the AIS at controlling excitatory output, little is known about the behavioral impact of its loss. Here we report reduced α2 signaling at the AIS results in a drastic increase in baseline EEG delta power in *Gabra*2-1 homozygous mice. This finding extends previous observations of increased delta power in *Gabra*2-1 homozygous mice to a longer time scale (24 hours) as previous recordings were 1hr in duration and made while the animals were awake. In addition, by utilizing longer recording times we were able to discover that the increase in baseline delta power is not modulated with respect to the animal's circadian period. These findings suggest *Gabra*2-1 homozygous mice have altered brain wide processing.

Given the *Gabra*2-1 mouse model displayed an increase in delta frequencies which are predominate during the state of NR sleep, we next wished to parse out the specific impact of loss of α2 signaling at the AIS on sleep and sleep quality. Examination of 24 hour EEG recordings revealed the increased delta power observed in *Gabra*2-1 homozygous mice is restricted to the state of NR sleep while decreased gamma power is observed during the state of W. Although further measures are needed to determine the behavioral impact of reduced gamma power in *Gabra*2-1 homozygous mice during W, gamma power is associated with active learning and memory[7,89]. Further, altered gamma frequencies are often observed in psychiatric disorders and neurodevelopmental disorders[90–92]. In addition, high frequencies (30-100Hz) have been demonstrated to be dependent upon the activity of $GABA_ARs$ found at inhibitory

synaptic sites[93]. Given this, our observation of the *Gabra*2-1 mouse model suggests gamma frequencies during the state of W may depend upon α2 signaling at the AIS. Delta power is modulated by prior activity with extended wakefulness resulting in increased delta power[71]. As such, high delta during NR sleep is associated with high levels of sleep pressure[69]. Our data demonstrate *Gabra*2-1 homozygous mice have increased delta power restricted to the state of NR indicating they have a high level of baseline sleep pressure. Interestingly, high sleep pressure (delta) does not correlate to good sleep quality as people with Rett's syndrome, who demonstrate continuous high delta activity, have been shown to have poor sleep efficiency[94].

Because we detected several baseline measures altered that are associated with sleep and sleep quality, we next examined the distribution of vigilance in the *Gabra*2-1 mice across an entire circadian cycle. We observed a similar amount of time spend in a state of W, NR, or R when examining the 24 hour period, yet when parsed by subjective day and night we find altered distribution of these states. Specifically, we find an increase in time spend awake during subjective night. Further, we found dysregulation amongst the relationship between delta and theta frequencies occurring primarily 2 hours before and after the day/night transition. Data from the human population suggests sleep onset is depended on the reduction of high frequency's associated with wakefulness (beta, alpha, gamma) and an increase in the low frequencies associated with sleep (delta and theta)[95]. Therefore, the dysregulation of delta to theta observed in *Gabra*2-1 homozygous may be mechanistic in our findings that they have difficulty patterning vigilance around the circadian cycle. These data suggest the observed

baseline EEG alterations have a significant impact on the homeostatic progression of sleep in *Gabra*2-1 mice.

Having established an increase in time spent awake during subjective night along with an indication of poor regulation of vigilance state transitions (dysregulated delta/theta) in *Gabra*2-1 homozygous mice, we next set out to examine vigilance state transitions across the 24 hour period. When examining all vigilance state transition types (W to NR, NR to W, NR to R, and NR to R) we report an overall deficit in vigilance state transitioning in *Gabra*2-1 homozygous mice that is restricted to subjective night. Further, when parsed by transition type, we find the deficit in transitioning is restricted to the transitions from NR sleep into R sleep or from R sleep back into NR sleep (NR-R-NR). The NR-R-NR transitions are a relatively well described process that depend on inhibition or disinhibition at appropriate times of several brain regions including the pontine nuclei[96,97]. Of note, the pontine nuclei is found to be highly enriched with α2[20]. In addition, in humans it has been demonstrated that the onset of REM sleep is preceded by a decrease in delta and theta power and the inverse is true for its offset[98]. Our data suggests reduced α2 at the AIS increases baseline delta power, altering the relationship amongst the delta and theta frequencies and as such may contribute to the observed difficulty in the NR-R-NR transition.

Having established baseline alterations in *Gabra*2-1 homozygous EEG activity, vigilance state patterning, and vigilance state transitioning, we set out to confirm these observations by introducing sleep challenges. It is well known that some sleep disorders are associated with difficulty maintaining circadian rhythmicity and coping with challenges to sleep[99,100]. Thus, if the *Gabra*2-1 mice are having difficulty with sleep

patterning, we would expect to see an altered homeostatic response to sleep challenges. Here we report a deficit in *Gabra*2-1 homozygous mice ability to maintain a circadian rhythm in the absences of the salient environmental zeitgeber light. This deficit may be considered severe as we observed a loss of rhythmicity in a brief period of time (1 to 2 days of constant darkness) while the wildtype mice maintained a free running rhythm for the entirety of the experiment. Further supporting our findings of sleep deficits in *Gabra*2-1 homozygous mice, here we report an attenuated homoeostatic response to SD. As mentioned above, it is a well-known phenomenon that sleep pressure is dependent upon prior activity thus, SD increases sleep pressure[69,71]. Given Gabra2-1 homozygous mice underwent SD similar to wildtype controls (~95% W of 24 hours SD) it is striking to report an inability of these mice to homeostatically alter vigilance state patterning (increase time asleep) as little to no change occurred in response to SD. These data taken together demonstrate the *Gabra2*-1 homozygous mice have difficulty homeostatically responding to sleep challenges and support our claims of baseline homeostatic dysregulation.

In conclusion, our findings reveal the role of $GABA_A$ receptors containing the α2 subunit found enriched at the AIS postsynaptic to chandelier cells to the establishment, maintenance, and quality of sleep. We demonstrate that a loss of GABAergic signaling at the AIS results in an overall increase in EEG delta frequencies that are maintained across the circadian cycle. We find this increase in delta power is accompanied by alterations to vigilance state patterning, specifically, a reduction in time asleep during subjective night. Lastly, we report an altered response to two different sleep challenges in *Gabra*2-1 mice, supporting our findings of poor-quality baseline sleep. These data

begin to shed light on the molecular mechanisms of common sleep disturbances observed in humans known to have altered GABAergic. Further these data will provide insight for the development of targeted sleep therapeutics.

To conclude this project, we are currently undertaking experiments using IHC to examine $GABA_A$Rs containing the α2 subunit in the tuberomammillary nucleus of *Gabra*2-1 mice. The tuberomammillary nucleus houses histaminergic neurons that are active during W and inactive during states of sleep. GABAergic neurons projecting from the preoptic nucleus drive this sleep wake profile of histaminergic neurons. We suspect a reduction of α2 receptors in the tuberomammillary nucleus may be mechanistic to the homeostatic dysregulation of sleep observed in *Gabra*2-1 mice.

CHAPTER 7

SUPPLEMENTARY INFORMATION

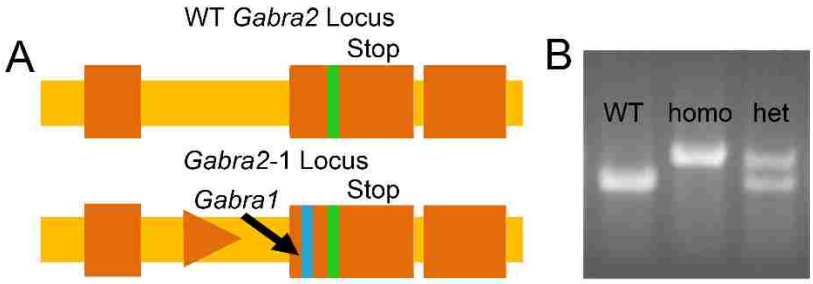

Supplementary Figure 1. Generation and genotyping *Gabra2*-1 mice.

A. Cartoon schematic depicting the targeting vector used to insert amino acid residues 358-375 form the large intercellular α1 loop into exon 10 of the α2 subunit. B. Representative polymerase change reaction results for identification of wildtype littermate controls, *Gabra2*-1 heterozygous (het), and *Gabra2*-1 homozygous (homo) mice.

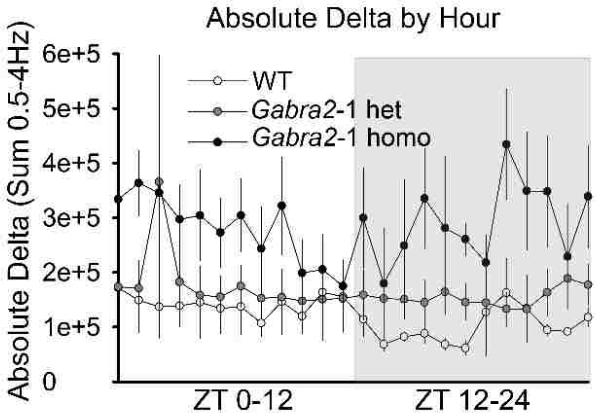

Supplementary Figure 2. Hourly assessment of absolute delta power for a 24 hour period.

Summation of total power in frequencies from 0.5-4Hz hrouly for 24 hours suggests consistently elevated power in *Gabra2*-1 homozygous mice across the circadian cycle (LS means; WT – 121571.135 ± 48565.020; het – 166484.957 ± 43437.874; homo – 287123.257 ± 48565.020) n = 4 to 5 per genotype; values listed are mean ± standard error; p values from repeated measures ANOVA, post hoc Bonferroni; * = ⩽0.05, ** = ⩽0.005, *** = <0.001.

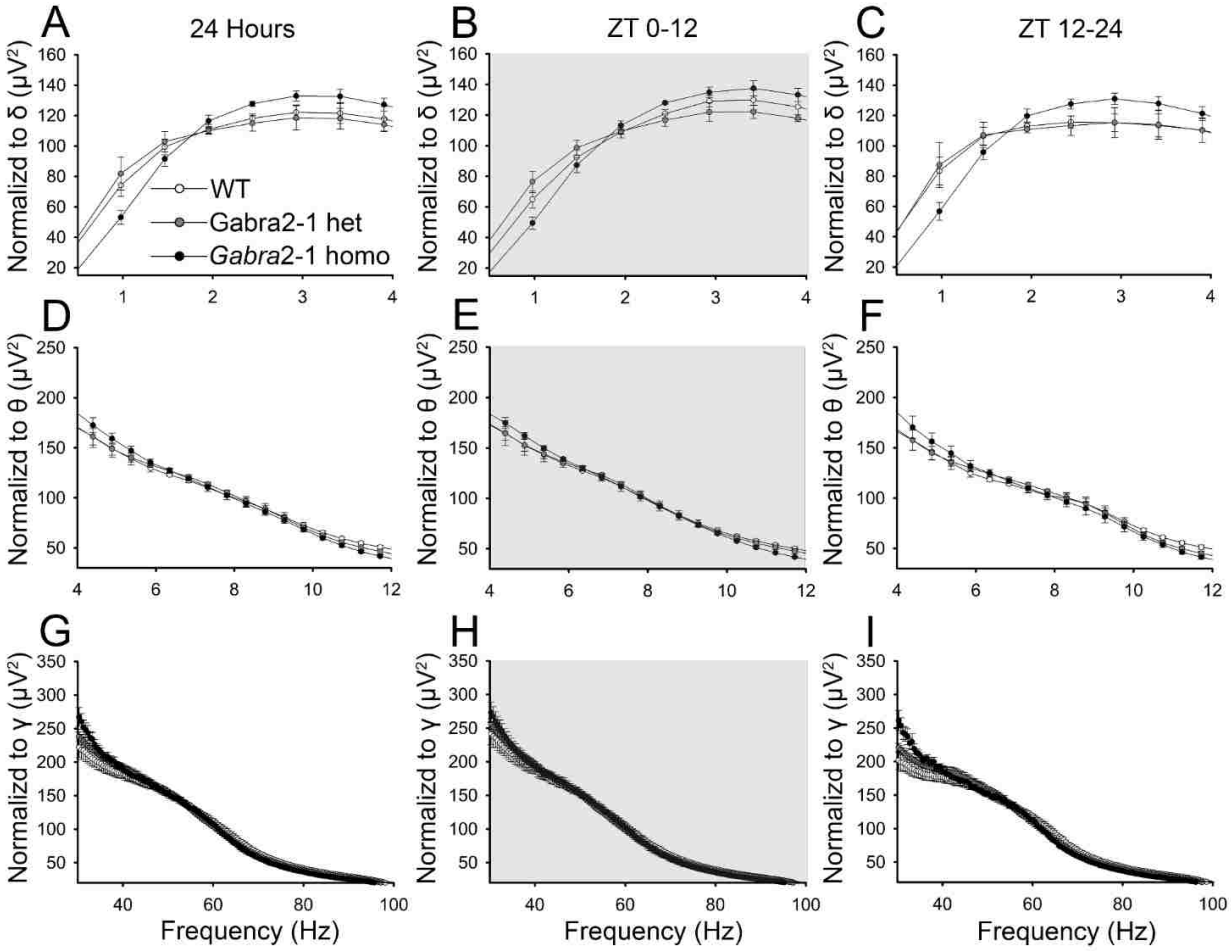

Supplemental Figure 3. 24 hour cFFT normalized to delta, theta, and gamma.

A-C. Cumulative fast fourier transformation (cFFT) applied to 24 hours EEG data and normalized to average δ power for 24 hour period (A), Zeitgeber time (ZT) 0-12 (B), and ZT 12-24 (C). D-F. Cumulative fast Fourier transformation (cFFT) applied to 24 hours EEG data and normalized to average θ power for 24 hour period (D), ZT 0-12 (E), and ZT 12-24 (F). G-I. Cumulative fast Fourier transformation (cFFT) applied to 24 hours EEG data and normalized to average γ power for 24 hour period (G), ZT 0-12 (H), and ZT 12-24 (I).

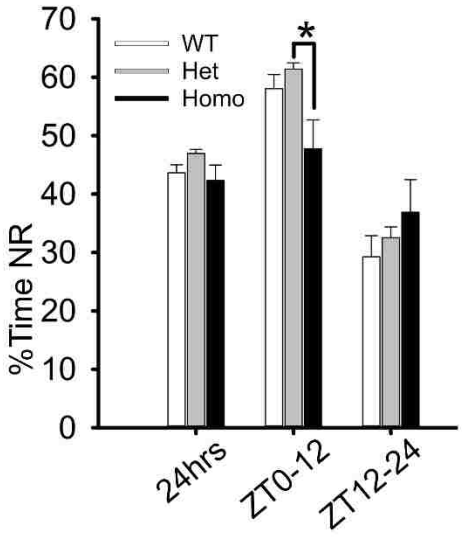

Supplementary Figure 4. Assessment of percent time spent in state of non-rapid-eye-movement sleep.

Values expressed as a percent of total analysis time (24 hours, zeitgeber time (ZT) 0-12, and ZT 12-24). n = 4 to 5 per genotype; values listed are mean ± standard error; p values from repeated measures ANOVA, post hoc Bonferroni; * = ⩽0.05, ** = ⩽0.005, *** = <0.001.

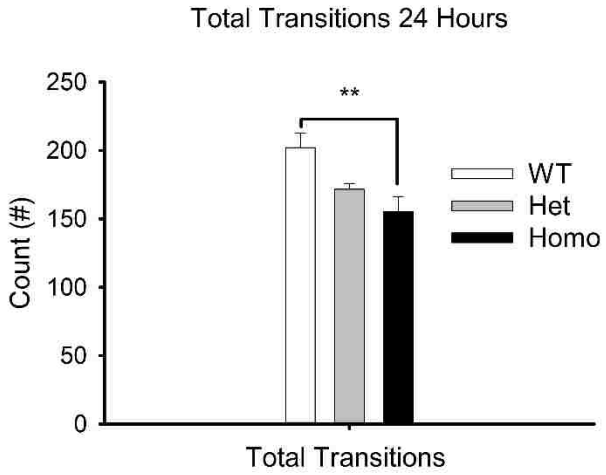

Supplementary Figure 5. Assessment of total transitions across a 24 hour period.

Summation of all transition types (W to NR, NR to W, NR to R, and R to NR) across a 24 hour period demonstrates a significant reduction in *Gabra2*-1 homozygous mice vigilance state transitioning. n = 4 to 5 per genotype; values listed are mean ± standard error; p values from one way ANOVA, post hoc Bonferroni; * = ⩽0.05, ** = ⩽0.005, *** = <0.001.

Modality/Assessment	Wildtype	Het	Homo
Visual Placement	Normal	Normal	Normal
Corneal Reflex	Normal	Normal	Normal

Supplementary Table 1. Results for two visual tests from modified SHIRPA screening protocols.

BIBLIOGRAPHY

1. Benington, J. H. Sleep homeostasis and the function of sleep. *Sleep* **23**, 959–966 (2000).
2. Colten, H. R., Altevogt, B. M. & Research, I. of M. (US) C. on S. M. and. *Extent and Health Consequences of Chronic Sleep Loss and Sleep Disorders*. (National Academies Press (US), 2006).
3. Ju, Y.-E. S., Videnovic, A. & Vaughn, B. V. Comorbid Sleep Disturbances in Neurologic Disorders. *Contin. Minneap. Minn* **23**, 1117–1131 (2017).
4. Borbély, A. A. A two process model of sleep regulation. *Hum. Neurobiol.* **1**, 195–204 (1982).
5. Takahashi, J. S., Hong, H.-K., Ko, C. H. & McDearmon, E. L. The genetics of mammalian circadian order and disorder: implications for physiology and disease. *Nat. Rev. Genet.* **9**, 764–775 (2008).
6. Kleitman, N. Basic rest-activity cycle--22 years later. *Sleep* **5**, 311–317 (1982).
7. Sejnowski, T. J. & Destexhe, A. Why do we sleep? *Brain Res.* **886**, 208–223 (2000).
8. Montgomery, S. M., Sirota, A. & Buzsáki, G. Theta and gamma coordination of hippocampal networks during waking and REM sleep. *J. Neurosci. Off. J. Soc. Neurosci.* **28**, 6731–6741 (2008).
9. Chung, S. *et al.* Identification of preoptic sleep neurons using retrograde labelling and gene profiling. *Nature* **545**, 477–481 (2017).
10. Wisden, W., Yu, X. & Franks, N. P. GABA Receptors and the Pharmacology of Sleep. 1–26 (2017). doi:10.1007/164_2017_56
11. Möhler, H., Crestani, F. & Rudolph, U. GABAA-receptor subtypes: a new pharmacology. *Curr. Opin. Pharmacol.* **1**, 22–25 (2001).
12. Rudolph, U. *et al.* Benzodiazepine actions mediated by specific gamma-aminobutyric acid(A) receptor subtypes. *Nature* **401**, 796–800 (1999).
13. Scammell, T. E., Arrigoni, E. & Lipton, J. Neural Circuitry of Wakefulness and Sleep. *Neuron* **93**, 747–765 (2017).
14. Sieghart, W. & Sperk, G. Subunit composition, distribution and function of GABA(A) receptor subtypes. *Curr. Top. Med. Chem.* **2**, 795–816 (2002).
15. Ali Rodriguez, R., Joya, C. & Hines, R. M. Common Ribs of Inhibitory Synaptic Dysfunction in the Umbrella of Neurodevelopmental Disorders. *Front. Mol. Neurosci.* **11**, (2018).
16. Preserving the balance: diverse forms of long-term GABAergic synaptic plasticity | Nature Reviews Neuroscience. (2019). Available at: https://www.nature.com/articles/s41583-019-0141-5. (Accessed: 9th April 2019)
17. Brown, R. E., Basheer, R., McKenna, J. T., Strecker, R. E. & McCarley, R. W. CONTROL OF SLEEP AND WAKEFULNESS. *Physiol. Rev.* **92**, 1087–1187 (2012).
18. Gottesmann, C. GABA mechanisms and sleep. *Neuroscience* **111**, 231–239 (2002).
19. Clark, B. D., Goldberg, E. M. & Rudy, B. Electrogenic Tuning of the Axon Initial Segment. *Neurosci. Rev. J. Bringing Neurobiol. Neurol. Psychiatry* **15**, 651–668 (2009).

20. Mozrzymas, J. W., Zarnowska, E. D., Pytel, M., Mercik, K. & Zarmowska, E. D. Modulation of GABA(A) receptors by hydrogen ions reveals synaptic GABA transient and a crucial role of the desensitization process. *J. Neurosci. Off. J. Soc. Neurosci.* **23**, 7981–7992 (2003).
21. Tretter, V., Ehya, N., Fuchs, K. & Sieghart, W. Stoichiometry and Assembly of a Recombinant GABAA Receptor Subtype. *J. Neurosci.* **17**, 2728–2737 (1997).
22. Klausberger, T., Roberts, J. D. B. & Somogyi, P. Cell Type- and Input-Specific Differences in the Number and Subtypes of Synaptic GABAA Receptors in the Hippocampus. *J. Neurosci.* **22**, 2513–2521 (2002).
23. Klausberger, T. & Somogyi, P. Neuronal Diversity and Temporal Dynamics: The Unity of Hippocampal Circuit Operations. *Science* **321**, 53–57 (2008).
24. Leterrier, C. The Axon Initial Segment: An Updated Viewpoint. *J. Neurosci. Off. J. Soc. Neurosci.* **38**, 2135–2145 (2018).
25. Nusser, Z., Sieghart, W., Benke, D., Fritschy, J. M. & Somogyi, P. Differential synaptic localization of two major gamma-aminobutyric acid type A receptor alpha subunits on hippocampal pyramidal cells. *Proc. Natl. Acad. Sci. U. S. A.* **93**, 11939–11944 (1996).
26. Somogyi, P., Tamás, G., Lujan, R. & Buhl, E. H. Salient features of synaptic organisation in the cerebral cortex. *Brain Res. Brain Res. Rev.* **26**, 113–135 (1998).
27. Grubb, M. S. *et al.* Short- and long-term plasticity at the axon initial segment. *J. Neurosci. Off. J. Soc. Neurosci.* **31**, 16049–16055 (2011).
28. Rowlett, J. K., Platt, D. M., Lelas, S., Atack, J. R. & Dawson, G. R. Different GABAA receptor subtypes mediate the anxiolytic, abuse-related, and motor effects of benzodiazepine-like drugs in primates. *Proc. Natl. Acad. Sci. U. S. A.* **102**, 915–920 (2005).
29. Kopp, C., Rudolph, U. & Tobler, I. Sleep EEG changes after zolpidem in mice. *Neuroreport* **15**, 2299–2302 (2004).
30. Uygun, D. S. *et al.* Bottom-Up versus Top-Down Induction of Sleep by Zolpidem Acting on Histaminergic and Neocortex Neurons. *J. Neurosci. Off. J. Soc. Neurosci.* **36**, 11171–11184 (2016).
31. Bäckberg, M., Ultenius, C., Fritschy, J.-M. & Meister, B. Cellular localization of GABA receptor alpha subunit immunoreactivity in the rat hypothalamus: relationship with neurones containing orexigenic or anorexigenic peptides. *J. Neuroendocrinol.* **16**, 589–604 (2004).
32. Fritschy, J. M. & Mohler, H. GABAA-receptor heterogeneity in the adult rat brain: differential regional and cellular distribution of seven major subunits. *J. Comp. Neurol.* **359**, 154–194 (1995).
33. Sergeeva, O. A., Andreeva, N., Garret, M., Scherer, A. & Haas, H. L. Pharmacological properties of GABAA receptors in rat hypothalamic neurons expressing the epsilon-subunit. *J. Neurosci. Off. J. Soc. Neurosci.* **25**, 88–95 (2005).
34. Tretter, V. *et al.* Deficits in spatial memory correlate with modified γ-aminobutyric acid type A receptor tyrosine phosphorylation in the hippocampus. *Proc. Natl. Acad. Sci.* **106**, 20039–20044 (2009).
35. Hines, R. M. *et al.* Developmental seizures and mortality result from reducing GABAA receptor α2-subunit interaction with collybistin. *Nat. Commun.* **9**, (2018).

36. Bowery, N. G. & Smart, T. G. GABA and glycine as neurotransmitters: a brief history. *Br. J. Pharmacol.* **147**, S109–S119 (2006).
37. Erlander, M. G., Tillakaratne, N. J., Feldblum, S., Patel, N. & Tobin, A. J. Two genes encode distinct glutamate decarboxylases. *Neuron* **7**, 91–100 (1991).
38. Trist, D. G., Kenakin, T. P. & Blackburn, T. P. In memory of Norman Bowery (1944-2016). *Curr. Opin. Pharmacol.* **35**, 89–93 (2017).
39. Benarroch, E. E. GABAB receptors: structure, functions, and clinical implications. *Neurology* **78**, 578–584 (2012).
40. Tiao, J. Y.-H. & Bettler, B. Characteristics of GABA<Subscript>B</Subscript> Receptor Mutant Mice. in *The GABA Receptors* 273–287 (Humana Press, 2007). doi:10.1007/978-1-59745-465-0_11
41. Sieghart, W. Structure and pharmacology of gamma-aminobutyric acidA receptor subtypes. *Pharmacol. Rev.* **47**, 181–234 (1995).
42. Sieghart, W. & Sperk, G. Subunit composition, distribution and function of GABA(A) receptor subtypes. *Curr. Top. Med. Chem.* **2**, 795–816 (2002).
43. Kole, M. H. P. & Stuart, G. J. Signal processing in the axon initial segment. *Neuron* **73**, 235–247 (2012).
44. Brown, N., Kerby, J., Bonnert, T. P., Whiting, P. J. & Wafford, K. A. Pharmacological characterization of a novel cell line expressing human α4β3δ GABAA receptors. *Br. J. Pharmacol.* **136**, 965–974 (2002).
45. Haas, K. F. & Macdonald, R. L. GABAA receptor subunit gamma2 and delta subtypes confer unique kinetic properties on recombinant GABAA receptor currents in mouse fibroblasts. *J. Physiol.* **514 (Pt 1)**, 27–45 (1999).
46. Lewis, D. A., Hashimoto, T. & Volk, D. W. Cortical inhibitory neurons and schizophrenia. *Nat. Rev. Neurosci.* **6**, 312–324 (2005).
47. Kneussel, M. *et al.* Loss of postsynaptic GABA(A) receptor clustering in gephyrin-deficient mice. *J. Neurosci. Off. J. Soc. Neurosci.* **19**, 9289–9297 (1999).
48. Kneussel, M. *et al.* The gamma-aminobutyric acid type A receptor (GABAAR)-associated protein GABARAP interacts with gephyrin but is not involved in receptor anchoring at the synapse. *Proc. Natl. Acad. Sci. U. S. A.* **97**, 8594–8599 (2000).
49. Mukherjee, J. *et al.* The residence time of GABA(A)Rs at inhibitory synapses is determined by direct binding of the receptor α1 subunit to gephyrin. *J. Neurosci. Off. J. Soc. Neurosci.* **31**, 14677–14687 (2011).
50. Tretter, V. *et al.* The clustering of GABA(A) receptor subtypes at inhibitory synapses is facilitated via the direct binding of receptor alpha 2 subunits to gephyrin. *J. Neurosci. Off. J. Soc. Neurosci.* **28**, 1356–1365 (2008).
51. Tretter, V. *et al.* Molecular basis of the γ-aminobutyric acid A receptor α3 subunit interaction with the clustering protein gephyrin. *J. Biol. Chem.* **286**, 37702–37711 (2011).
52. Cajal, S. R. *et al.* Estructura de los centros nerviosos de las aves. (1888).
53. Yuste, R. From the neuron doctrine to neural networks. *Nat. Rev. Neurosci.* **16**, 487–497 (2015).
54. Hodgkin, A. L. & Huxley, A. F. A quantitative description of membrane current and its application to conduction and excitation in nerve. *J. Physiol.* **117**, 500–544 (1952).

55. Van Wart, A., Trimmer, J. S. & Matthews, G. Polarized distribution of ion channels within microdomains of the axon initial segment. *J. Comp. Neurol.* **500**, 339–352 (2007).
56. Lorincz, A. & Nusser, Z. Cell-Type-Dependent Molecular Composition of the Axon Initial Segment. *J. Neurosci.* **28**, 14329–14340 (2008).
57. Royeck, M. *et al.* Role of axonal NaV1.6 sodium channels in action potential initiation of CA1 pyramidal neurons. *J. Neurophysiol.* **100**, 2361–2380 (2008).
58. Dodson, P. D., Barker, M. C. & Forsythe, I. D. Two heteromeric Kv1 potassium channels differentially regulate action potential firing. *J. Neurosci. Off. J. Soc. Neurosci.* **22**, 6953–6961 (2002).
59. Somogyi, P. A specific 'axo-axonal' interneuron in the visual cortex of the rat. *Brain Res.* **136**, 345–350 (1977).
60. Tai, Y., Gallo, N. B., Wang, M., Yu, J.-R. & Van Aelst, L. Axo-axonic Innervation of Neocortical Pyramidal Neurons by GABAergic Chandelier Cells Requires AnkyrinG-Associated L1CAM. *Neuron* (2019). doi:10.1016/j.neuron.2019.02.009
61. Tai, Y., Janas, J. A., Wang, C.-L. & Van Aelst, L. Regulation of chandelier cell cartridge and bouton development via DOCK7-mediated ErbB4 activation. *Cell Rep.* **6**, 254–263 (2014).
62. Inan, M. *et al.* Dense and overlapping innervation of pyramidal neurons by neocortical chandelier cells. *J. Neurosci. Off. J. Soc. Neurosci.* **33**, 1907–1914 (2013).
63. Ribak, C. E. Axon terminals of GABAergic chandelier cells are lost at epileptic foci. *Brain Res.* **326**, 251–260 (1985).
64. Rubenstein, J. L. R. & Merzenich, M. M. Model of autism: increased ratio of excitation/inhibition in key neural systems. *Genes Brain Behav.* **2**, 255–267 (2003).
65. Ariza, J., Rogers, H., Hashemi, E., Noctor, S. C. & Martínez-Cerdeño, V. The Number of Chandelier and Basket Cells Are Differentially Decreased in Prefrontal Cortex in Autism. *Cereb. Cortex N. Y. N 1991* **28**, 411–420 (2018).
66. Volk, D. W. *et al.* Reciprocal alterations in pre- and postsynaptic inhibitory markers at chandelier cell inputs to pyramidal neurons in schizophrenia. *Cereb. Cortex N. Y. N 1991* **12**, 1063–1070 (2002).
67. Massi, L. *et al.* Temporal Dynamics of Parvalbumin-Expressing Axo-axonic and Basket Cells in the Rat Medial Prefrontal Cortex In Vivo. *J. Neurosci. Off. J. Soc. Neurosci.* **32**, 16496–16502 (2012).
68. Aschoff, J. Circadian Rhythms in Man: A self-sustained oscillator with an inherent frequency underlies human 24-hour periodicity. *Science* **148**, 1427–1432 (1965).
69. McKenna, J. T. *et al.* Sleep fragmentation elevates behavioral, electrographic and neurochemical measures of sleepiness. *Neuroscience* **146**, 1462–1473 (2007).
70. Rodriguez, A. V. *et al.* Why Does Sleep Slow-Wave Activity Increase After Extended Wake? Assessing the Effects of Increased Cortical Firing During Wake and Sleep. *J. Neurosci. Off. J. Soc. Neurosci.* **36**, 12436–12447 (2016).
71. Suzuki, A., Sinton, C. M., Greene, R. W. & Yanagisawa, M. Behavioral and biochemical dissociation of arousal and homeostatic sleep need influenced by prior wakeful experience in mice. *Proc. Natl. Acad. Sci. U. S. A.* **110**, 10288–10293 (2013).

72. Mazuski, C. *et al.* Entrainment of Circadian Rhythms Depends on Firing Rates and Neuropeptide Release of VIP SCN Neurons. *Neuron* **99**, 555-563.e5 (2018).
73. Kräuchi, K. & Wirz-Justice, A. Circadian clues to sleep onset mechanisms. *Neuropsychopharmacol. Off. Publ. Am. Coll. Neuropsychopharmacol.* **25**, S92-96 (2001).
74. Kleitman, N. *Sleep and wakefulness*. (Univ. Chicago Press, 1963).
75. Sherin, J. E., Shiromani, P. J., McCarley, R. W. & Saper, C. B. Activation of ventrolateral preoptic neurons during sleep. *Science* **271**, 216–219 (1996).
76. Thalamocortical oscillations in the sleeping and aroused brain. - PubMed - NCBI. Available at: https://www.ncbi.nlm.nih.gov/pubmed/8235588. (Accessed: 19th April 2019)
77. Saper, C. B., Chou, T. C. & Scammell, T. E. The sleep switch: hypothalamic control of sleep and wakefulness. *Trends Neurosci.* **24**, 726–731 (2001).
78. Brunner, D. P., Dijk, D.-J., Münch, M. & Borbély, A. A. Effect of zolpidem on sleep and sleep EEG spectra in healthy young men. *Psychopharmacology (Berl.)* **104**, 1–5 (1991).
79. Bäckberg, M., Ultenius, C., Fritschy, J.-M. & Meister, B. Cellular Localization of GABAA Receptor α Subunit Immunoreactivity in the Rat Hypothalamus: Relationship With Neurones Containing Orexigenic or Anorexigenic Peptides. *J. Neuroendocrinol.* **16**, 589–604 (2004).
80. Wisden, W., Laurie, D. J., Monyer, H. & Seeburg, P. H. The distribution of 13 GABAA receptor subunit mRNAs in the rat brain. I. Telencephalon, diencephalon, mesencephalon. *J. Neurosci. Off. J. Soc. Neurosci.* **12**, 1040–1062 (1992).
81. May, A. C., Fleischer, W., Kletke, O., Haas, H. L. & Sergeeva, O. A. Benzodiazepine-site pharmacology on GABAA receptors in histaminergic neurons. *Br. J. Pharmacol.* **170**, 222–232 (2013).
82. Vyazovskiy, V. V. & Tobler, I. Regional differences in NREM sleep slow-wave activity in mice with congenital callosal dysgenesis. *J. Sleep Res.* **14**, 299–304 (2005).
83. de Andrés, I., Garzón, M. & Reinoso-Suárez, F. Functional Anatomy of Non-REM Sleep. *Front. Neurol.* **2**, (2011).
84. Weiergräber, M., Henry, M., Hescheler, J., Smyth, N. & Schneider, T. Electrocorticographic and deep intracerebral EEG recording in mice using a telemetry system. *Brain Res. Brain Res. Protoc.* **14**, 154–164 (2005).
85. Vassalli, A. & Franken, P. Hypocretin (orexin) is critical in sustaining theta/gamma-rich waking behaviors that drive sleep need. *Proc. Natl. Acad. Sci.* **114**, E5464–E5473 (2017).
86. Liu, X.-G., Zhang, B.-J., Xu, X.-H., Huang, Z.-L. & Qu, W.-M. Lesions of suprachiasmatic nucleus modify sleep structure but do not alter the total amount of daily sleep in rats. *Sleep Biol. Rhythms* **10**, 293–301 (2012).
87. Stephenson, R., Lim, J., Famina, S., Caron, A. M. & Dowse, H. B. Sleep-Wake Behavior in the Rat: Ultradian Rhythms in a Light-Dark Cycle and Continuous Bright Light. *J. Biol. Rhythms* **27**, 490–501 (2012).
88. Eckel-Mahan, K. & Sassone-Corsi, P. Phenotyping Circadian Rhythms in Mice. *Curr. Protoc. Mouse Biol.* **5**, 271–281 (2015).

89. Bartos, M., Vida, I. & Jonas, P. Synaptic mechanisms of synchronized gamma oscillations in inhibitory interneuron networks. *Nat. Rev. Neurosci.* **8**, 45–56 (2007).
90. An, K. *et al.* Altered Gamma Oscillations during Motor Control in Children with Autism Spectrum Disorder. *J. Neurosci.* **38**, 7878–7886 (2018).
91. Fitzgerald, P. J. & Watson, B. O. Gamma oscillations as a biomarker for major depression: an emerging topic. *Transl. Psychiatry* **8**, (2018).
92. Williams, S. & Boksa, P. Gamma oscillations and schizophrenia. *J. Psychiatry Neurosci. JPN* **35**, 75–77 (2010).
93. Kalemaki, K., Konstantoudaki, X., Tivodar, S., Sidiropoulou, K. & Karagogeos, D. Mice With Decreased Number of Interneurons Exhibit Aberrant Spontaneous and Oscillatory Activity in the Cortex. *Front. Neural Circuits* **12**, 96 (2018).
94. Ammanuel, S. *et al.* Heightened Delta Power during Slow-Wave-Sleep in Patients with Rett Syndrome Associated with Poor Sleep Efficiency. *PLoS ONE* **10**, (2015).
95. De Gennaro, L., Ferrara, M. & Bertini, M. The boundary between wakefulness and sleep: quantitative electroencephalographic changes during the sleep onset period. *Neuroscience* **107**, 1–11 (2001).
96. McCARLEY, R. W. & Massaquoi, S. G. Neurobiological structure of the revised limit cycle reciprocal interaction model of REM cycle control. *J. Sleep Res.* **1**, 132–137 (1992).
97. Steriade, M., Datta, S., Paré, D., Oakson, G. & Curró Dossi, R. C. Neuronal activities in brain-stem cholinergic nuclei related to tonic activation processes in thalamocortical systems. *J. Neurosci. Off. J. Soc. Neurosci.* **10**, 2541–2559 (1990).
98. Hadjiyannakis, K., Ogilvie, R. D., Alloway, C. E. & Shapiro, C. FFT analysis of EEG during stage 2-to-REM transitions in narcoleptic patients and normal sleepers. *Electroencephalogr. Clin. Neurophysiol.* **103**, 543–553 (1997).
99. Dodson, E. R. & Zee, P. C. Therapeutics for Circadian Rhythm Sleep Disorders. *Sleep Med. Clin.* **5**, 701–715 (2010).
100. Garbazza, C. *et al.* Non-24-Hour Sleep-Wake Disorder Revisited - A Case Study. *Front. Neurol.* **7**, 17 (2016).

CURRICULUM VITAE

Austin J. Boren

CONTACT INFORMATION

Email: Austin.John.Boren@gmail.com

EDUCATION

University of Nevada, Las Vegas; 2016-present
Doctoral program, Experimental Psychology Neuroscience Emphasis
Expected graduation: 2022
GPA: 3.6

University of Nevada Las Vegas; 2014–2016
Bachelor of arts degree, psychology
Graduation: December 2015
Psychology GPA: 3.7

College of Southern Nevada; 2013–2014
Area of study; psychology
Transferred to University of Nevada, Las Vegas

University of Nevada, Reno; 2006–2010
Area of study; philosophy
Transferred to College of Southern Nevada

RESEARCH EXPERIENCE

University of Nevada, Las Vegas Hines Group;

Fall 2017-Current
Title: Graduate Student
Faculty Advisor: Rochelle Hines Ph.D
Responsibilities:
· Murine electroencephalogram analysis and collection.
· Animal husbandry; breeding, weaning, and genotyping.

University of Nevada, Las Vegas Molecular and Behavioral Neuroscience Laboratory;

Fall 2016–Fall 2017
Title: Graduate Student
Faculty Advisor: Jefferson W. Kinney Ph.D.
Responsibilities:
· Behavioral assays including; Morris water maze, novel object recognition, open

field, tail flick, Barnes maze.
- Molecular assays including; Western blot, immunohistochemistry chemistry, end point polymerase chain reaction, protein concentration assay.
- Animal husbandry including; breeding, weaning, and genotyping.

University of Nevada, Las Vegas Molecular and Behavioral Neuroscience Laboratory;

Fall 2014–2015
Title: Undergraduate Research Assistant
Faculty Advisor: Jefferson W. Kinney Ph.D.
Responsibilities:
- Assisting in operation of behavioral assay including Morris water maze and forced swim task.
- Assisting in operation of biochemical assays including immunohistochemistry, Western blot, polymerase chain reaction, and protein concentration assay.
- Assisting in collecting tissue samples.
- Assisting in handling research animals.
- Organizing and conducting literature searches.

PROFESSIONAL PRESENTATIONS

1. **Austin Boren**, M. Khumnark, A. Contreras, D.J. Hines, R.M. Hines. Impared GA-BAergic signaling at the axon initial segment results in altered sleep architecture, bursting activity, and homeostatic sleep response. Society for Neuroscience 2018 poster presentation.

2. **Austin Boren,** Arnold Salazar, Andrew Murtishaw, Monica Bolton, Jefferson Kinney. GABA specific changes in a mouse model of Alzheimer's disease. Society for Neuroscience 2017 poster presentation.

3. Murtishaw, A.S**.,** Bolton, M.M., **Boren, A.J**., Salazar, A.M., Toughlian, J.E., Ortiz, A.A., Kinney, J.W. Alterations of high-fat diet in CX3CR1 knockout mice on neuroinflammation, metabolic markers, and Alzheimer's disease-related pathology. Society for the Study of Ingestive Behavior. Montreal, Canada, July 2017.

4. Murtishaw, A.S., Bolton, M.M., **Boren, A.J**., Salazar, A.M., Toughlian, J.E., Ortiz, A.A., Kinney, J.W. High-fat diet induced insulin disruption in CX3CR1 knockout mice on dementia-related pathology. Society for Neuroscience annual meeting. Washington, D.C., November 2017.

5. Andrew S. Murtishaw, Monica M. Bolton, **Austin J. Boren**, and Jefferson W. Kin ney. The effects of insulin impairments in CX3CR1 knockout mice on dementia-related pathology and neuroinflammation. Society for Neuroscience annual meeting. San Diego, CA, November 2016.

6. Murtishaw, A.S., Heaney, C.F., Bolton, M.M., Belmonte, K.C.D, Langardt, M.A., Calvin K.N., **Boren, A.J.,** & Kinney, J.W. A novel administration of systemic streptozotocin leads to alterations relevant to vascular dementia and Alzheimer's disease. Society for Neuroscience annual meeting. Chicago, IL, October 2015.

TEACHING EXPERINECE

Two sections Psychology 101 Spring 2019; instructor of records

Two sections Psychology 101 Fall 2018; instructor of records

CAMPUS ACTIVITIES AND LEADERSHIP

Sheep Brain Lab Demonstration for Psychology 101 Students; Spring 2019

Guest Speaker at Developmental Psychology Monthly Meeting; Fall 2018

Experimental psychology student council neuroscience emphases representative; 2017- 2018

Outreach Undergraduate Mentoring Program; 2017- 2018

Presenting member of Neuroscience Journal Club; 2014–present

Physiology of Psychology Tutor (PSY 303); Spring 2015

COMMUNITY OUTREACH

Side by side – Cleveland clinic; 2017
Yearly educational experience for high school students to observe neuropsychiatric evaluations at the Cleveland clinic.

Nevada brain bee board member; 2017
Yearly national competition for high school students on brain structure and function.

Brain awareness outreach; Spring 2015 – present
Educational presentations and workshops for elementary school children on brain function and safety.

AWARDS

Winner of Fall 2018 GPSA poster presentation forum

PROFESSIONAL REFERENCES

Rochelle Hines, Ph.D.
Assistant Professor, Department of Psychology, University of Nevada Las Vegas
4505 S. Maryland Parkway, CBC-C 5030 Las Vegas, NV 89154-0530.
Phone: 702-895-0187
Email: Rochelle.hines@unlv.edu

Dustin Hines, Ph.D.
Assistant Professor, Department of Psychology, University of Nevada Las Vegas
4505 S. Maryland Parkway, CBC-C 5030 Las Vegas, NV 89154-0530.
Phone: (702) 895-2208
Email: dustin.hines@unlv.edu

James M. Hyman, Ph.D.
Assistant Professor, Department of Psychology, University of Nevada Las Vegas
4505 S. Maryland Parkway, CBC-C 5030 Las Vegas, NV 89154-0530.
Phone: (702) 895-0109
Email: james.Hyman@unlv.edu